

HETEROCYCLES, Vol. 85, No. 6, 2012, pp. 1299 - 1332. © 2012 The Japan Institute of Heterocyclic Chemistry  
Received, 1st February, 2012, Accepted, 1st March, 2012, Published online, 5th March, 2012  
DOI: 10.3987/REV-12-732

## BIOACTIVE NATURAL PRODUCTS FROM MYXOMYCETES HAVING EFFECTS ON SIGNALING PATHWAYS

Masami Ishibashi\* and Midori A. Arai

Graduate School of Pharmaceutical Sciences, Chiba University, 1-8-1 Inohana, Chuo-ku, Chiba 260-8675, Japan. Email: mish@chiba-u.jp

**Abstract** – The myxomycetes (true slime molds) are an unusual group of primitive organisms that may be assigned to one of the lowest classes of eukaryotes. We studied the chemical constituents of a laboratory culture of plasmodia as well as field-collected fruit bodies of myxomycetes, and isolated various compounds with unique chemical structures and bioactivities. We recently also performed screening studies of natural products targeting signaling pathways related to basic studies of diseases and life sciences. Among myxomycetes constituents, we found several bioactive compounds that have effects on signaling pathways, including a cycloanthranilylproline with TRAIL resistance-overcoming activity, peptide lactone derivatives with Wnt signal inhibitory activity, a naphthoquinone pigment with Hes1 dimerization inhibition activity, and bisindole alkaloids with hedgehog signal inhibitory activity. Here we describe our recent results of their isolation, structure elucidation, synthesis, and findings in bioactivity studies.

### 1. INTRODUCTION

Natural products have played an important role in drug discovery for the treatment of various human diseases.<sup>1</sup> Eribulin, a synthetically prepared compound with a structure corresponding to the right-hand side of the sponge metabolite halichondrin B, was approved for the treatment of breast cancer in the USA in 2010 and in Europe and Japan in 2011.<sup>2</sup> Fingolimod (FTY720) was approved in the USA in 2010 for the treatment of multiple sclerosis, and the structure of this drug was inspired by the fungal metabolite myriocin, which was originally isolated as an antifungal agent and later identified as an immunosuppressant.<sup>3</sup> Among various natural product resources, prokaryotic and eukaryotic microorganisms have provided a wide variety of medicines and agrochemicals, starting with the

discovery of penicillin, but the vast majority of microorganisms remain unexplored as potential sources of new compounds.<sup>4</sup>

During our search for bioactive natural products, we have been investigating myxomycetes as an unexplored natural resource since 1998. Before our studies, there had been a limited number of explorative studies on the chemistry of myxomycetes by the groups of Steglich<sup>5</sup> and Asakawa.<sup>6</sup> We first studied a laboratory culture of myxomycetes on the basis of spore germination experiments of hundreds of field-collected fruit bodies collected in Japan and succeeded in laboratory culture of plasmodia of several myxomycetes on a practical scale for natural product chemistry studies, leading to the isolation of several unique metabolites, such as pyrroloiminoquinones and polyene yellow pigments from cultured plasmodia of *Didymium iridis* and *Physarum rigidum*, respectively. We also investigated field-collected fruit bodies of myxomycetes and isolated a number of new bioactive compounds, including naphthoquinone pigments and a cytotoxic triterpenoid aldehyde lactone from *Cribraria purpurea* and *Tubifera dimorphoteca*, respectively. We published other reviews on our studies of these myxomycete natural products several years ago.<sup>7-9</sup> An excellent review of secondary metabolites of myxomycetes was also described by Czech scientists in 2005.<sup>10</sup> In this review we describe more recent results of the studies of bioactive metabolites from myxomycetes and provide an update of the previous reviews.

We recently performed screening studies targeting signaling pathways which are related to basic studies of diseases and life sciences. Among the myxomycete metabolites, we found several bioactive compounds that affect signaling pathways.<sup>11,12</sup> This review therefore not only provides an update of the previous reviews but also deals with our recent results of screening studies using natural products isolated from myxomycetes as well as the synthesis of natural products and their related compounds.

The Myxomycetes (true slime molds) are an unusual group of primitive organisms that may be assigned to one of the lowest classes of eukaryote. In the assimilative phase of their life cycle (Figure 1) they form a free-living, multinucleate, acellular, mobile mass of protoplasm, called a plasmodium, which feeds on living bacteria. Under certain conditions, the plasmodium undergoes sporulation to develop into small, fungus-like fruit bodies which often have unique structures and colors. Spores, released from fruit bodies, germinate into protozoan-like myxamoeba, which mate to form a zygote which develops into the plasmodial stage.

We have examined laboratory-cultured plasmodial materials as well as field-collected fruit bodies to isolate natural products. Here we mainly describe four myxomycete natural products and their related compounds: (1) fuligocandins, cycloanthranilylprolines with TRAIL resistance-overcoming activity, (2) melleumins, peptide lactone derivatives with Wnt signal inhibitory activity, (3) lindbladione, a naphthoquinone pigment with Hes1 dimerization inhibition activity, and (4) arcyriflavins and related bisindole alkaloids with hedgehog signal inhibitory activity.

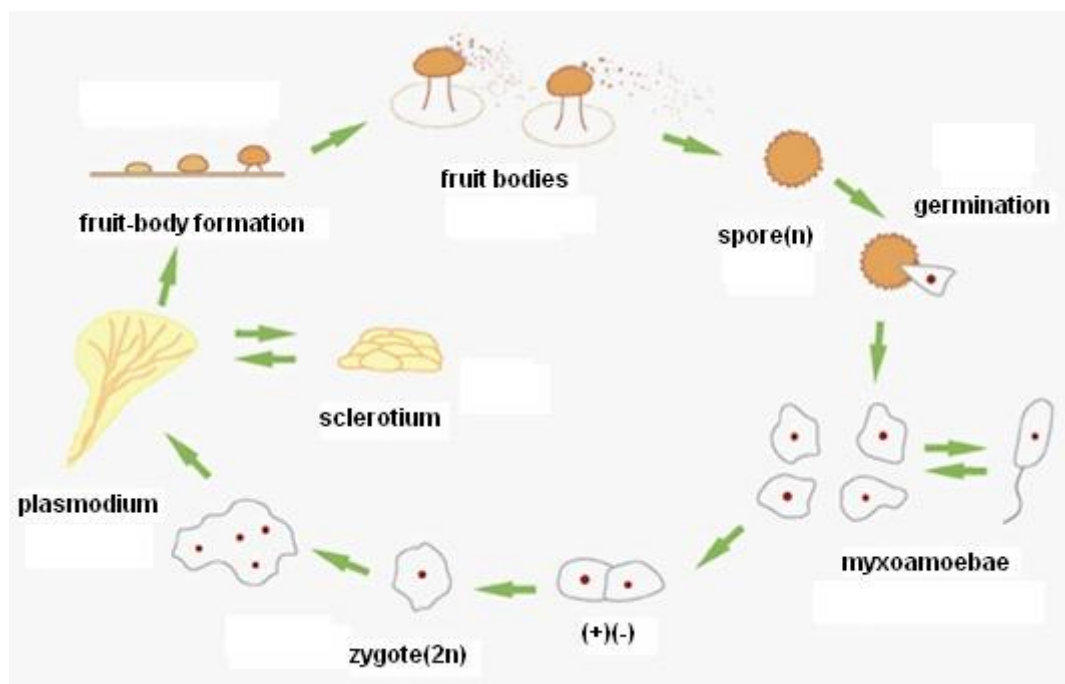


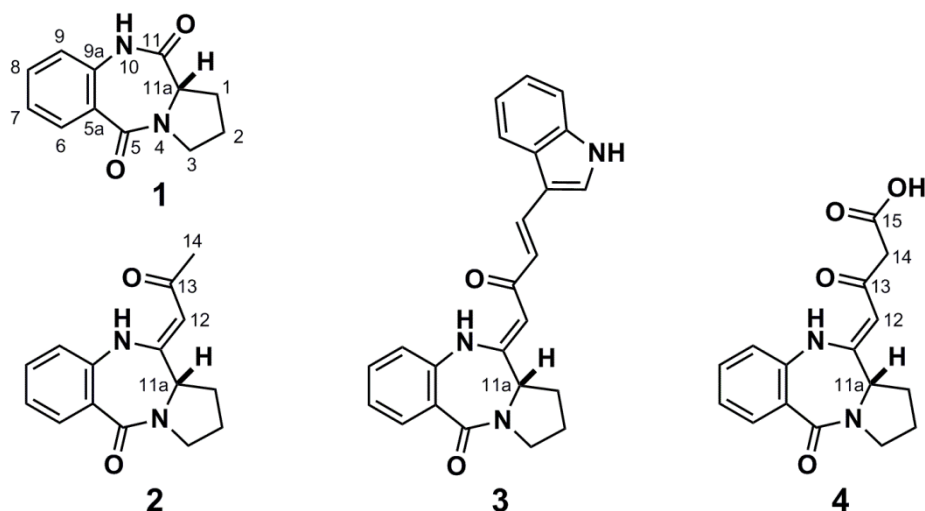
**Figure 1.** Lifecycle of myxomycetes

## 2. CYCLOANTHRANILYLPROLINES WITH TRAIL RESISTANCE-OVERCOMING ACTIVITY

The fruit bodies of *Fuligo candida* (Figure 2), collected in Motoyama-machi, Kochi Prefecture, Japan, were extracted with 90% MeOH and 90% acetone. The combined extracts were partitioned between EtOAc and water, and the EtOAc- soluble fraction was then subjected to chromatography on silica gel, ODS, and Sephadex LH-20 to give cycloanthranilylproline (**1**) and its derivatives, fuligo-candins A and B (**2** and **3**). From the water-soluble fraction, separation by ODS and silica gel flash chromatography along with reversed-phase HPLC afforded an unstable polar cycloanthranilylproline derivative, fuligocandin C (**4**).<sup>13</sup> Cycloanthranilylproline (**1**) was previously known, and was shown to contain L-proline from the comparison of optical rotation of **1** in the literature, which was previously obtained from a Cruciferous plant *Isatis indigotica*.<sup>14</sup>



**Figure 2.** Wild fruit bodies of *Fuligo candida*

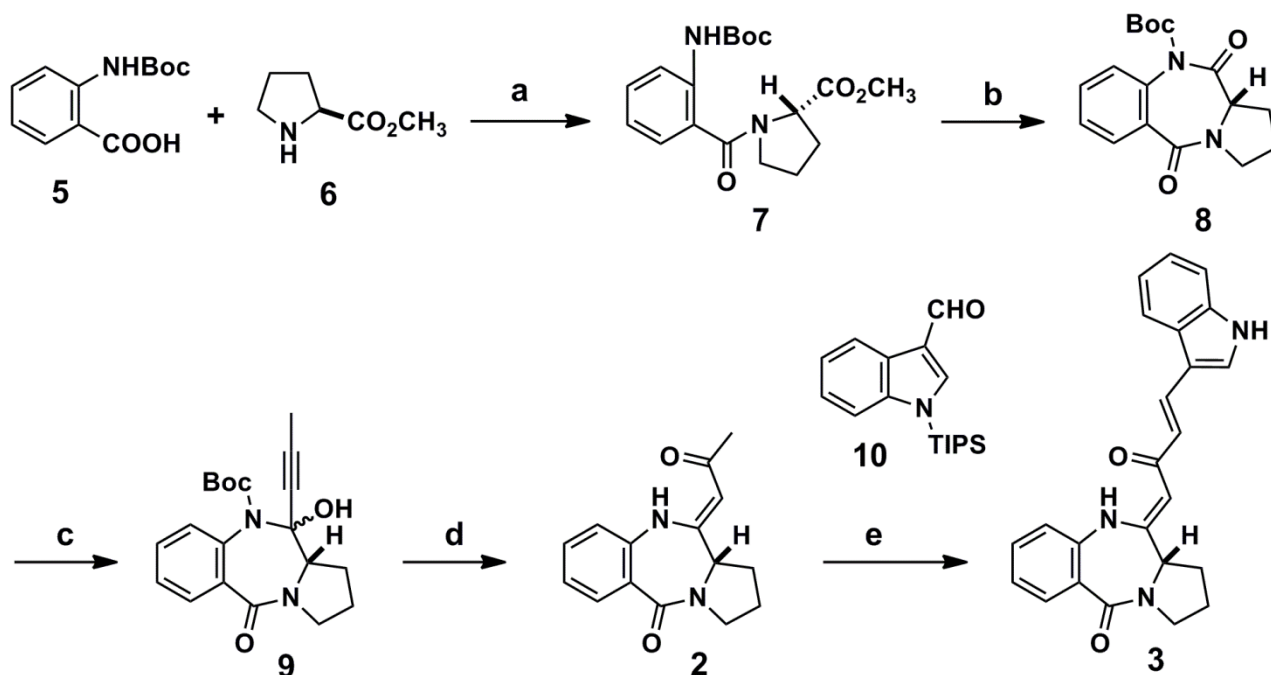


Spectral studies revealed that fuligocandin A (**2**) had a structure corresponding to that derived from condensation of **1** with acetone, and fuligocandin B (**3**) corresponded to that derived from condensation of **2** with indole-3-carbaldehyde. Fuligocandin C (**4**) was isolated from the water-soluble fraction, and was unstable and proved to be easily converted into fuligocandin A (**2**). The water-soluble fraction of this extract did not initially contain fuligocandin A (**2**); however, after ODS flash chromatography of the water-soluble fraction, fuligocandin A (**2**) was substantially obtained through decarboxylation of  $\beta$ -keto acid. Fuligocandin C (**4**) was isolated carefully by HPLC separation using Develosil C30-UG-5 eluted with 30% MeOH. In DMSO- $d_6$  solution, compound **4** was almost totally changed into compound **2** during the  $^1\text{H}$  NMR experiment. Since compound **4** was not dissolved in chloroform or acetone, NMR studies of compound **4** were carried out in  $\text{CD}_3\text{OD}$  solution, in which conversion from **4** to **2** was slow and not significantly observed. These observations suggested that fuligocandin A (**2**) was not artificially produced by condensation of cycloanthranilylproline (**1**) with acetone during acetone extraction; the methyl ketone moiety (C-12–C-14) of **2** is therefore not derived from acetone used for extraction but from the corresponding portion of fuligocandin C (**4**). It was likely that **2** was, at least partially, obtained from the  $\beta$ -keto acid (**4**) after extraction of this myxomycete, whereas it is also likely that the myxomycete organism contains fuligocandin A (**2**) as a natural product; decarboxylation may take place biogenetically or spontaneously inside the myxomycete's body before extraction.

Fuligocandin B (**3**) was meanwhile found as an active compound by a screening study for natural products that can overcome resistance to TRAIL, which was carried out by collaboration with H. Hasegawa, Nagasaki University, and K. Komiyama and M. Hayashi, Kitasato Institute.<sup>15</sup> Tumor necrosis factor (TNF)-related apoptosis-inducing ligand (TRAIL) induces apoptosis in many transformed cells; however, not all human tumors respond to TRAIL, potentially limiting its therapeutic utility. Nontoxic drugs that can augment sensitivity to TRAIL are therefore strongly demanded. Fuligocandin B

(**3**) was revealed to exhibit significant synergism with TRAIL.<sup>16</sup> Treatment of KOB cells (TRAIL-resistant Adult T-cell leukemia/lymphoma (ATLL) cell line) with fuligocandin B (**3**) and TRAIL resulted in apparent apoptosis, which was not induced by either agent alone. Four primary ATLL cells also showed an inhibition effect of cell proliferation by combined treatment with TRAIL and compound **3**, but normal peripheral blood mononuclear cells (PBMCs) were not affected at all by these treatments, thus implying that fuligocandin B (**3**) exhibited tumor-cell selective inhibition of cell proliferation in the presence of TRAIL. Combined treatment with TRAIL and fuligocandin B (**3**) activated caspase 8, 9, and 3; however, no significant change in expression of TRAIL receptors was observed in KOB cells treated with fuligocandin B (**3**), and the levels of apoptosis modulators such as Bax, Bak, Bcl-2, Bcl-xL, XIAP, cIAP-1, IAP-2, and survivin were not influenced by treatment with fuligocandin B (**3**). On the other hand, fuligocandin B (**3**) was found to increase the production of 15-deoxy- $\Delta^{12,14}$ -prostaglandin J<sub>2</sub> (15d-PGJ<sub>2</sub>) through activation of cyclooxygenase-2 (COX-2). 15d-PGJ<sub>2</sub> is an endogenous ligand of peroxisome proliferator-activated receptor- $\gamma$  (PPAR $\gamma$ ), and directly enhanced sensitivity to TRAIL by inhibiting antiapoptotic factors in several leukemia cell lines. This enhancement was regardless of PPAR $\gamma$  expression and was not blocked even by PPAR $\gamma$  siRNA, thus indicating that 15d-PGJ<sub>2</sub> sensitizes TRAIL-resistant cells to TRAIL in a PPAR $\gamma$ -independent manner and fuligocandin B (**3**), an inducer of 15d-PGJ<sub>2</sub>, may be useful as a new strategy for cancer therapy.

Since fuligocandin B (**3**) exhibited interesting bioactivity as above<sup>16</sup> and the absolute stereochemistry of the C-11a position of fuligocandins (**2** - **4**) had remained undetermined by spectral methods,<sup>13</sup> we studied the total synthesis of fuligocandins A and B (**2** and **3**). Total synthesis of fuligocandin A (**2**) was first reported by More *et al.* from azide derivatives,<sup>17</sup> and fuligocandins A and B (**2** and **3**) were also synthesized through the Eschenmoser coupling reaction of thione derivatives by Bergman *et al.*<sup>18</sup> These two syntheses, however, did not elucidate the absolute stereochemistry of fuligocandins. Our synthesis of fuligocandins A and B (**2** and **3**), as shown in Scheme 1, started with coupling *N*-Boc-anthranilic acid (**5**) with *L*-proline methyl ester (**6**) to give an amide **7**. Deprotection of the methyl ester of **7**, followed by intramolecular cyclization afforded *N*-Boc-cycloanthranilylproline **8**. Addition of propynyllithium to **8** afforded a single stereoisomer of propargylic alcohol **9**, which was subjected to Meyer-Schuster rearrangement with simultaneous deprotection of the Boc group under acidic conditions to give only the *Z*-isomer of fuligocandin A (**2**). Finally, according to Sunazuka's suggestion,<sup>16</sup> aldol condensation of **2** with indole aldehyde (**10**) and acidic deprotection of triisopropylsilyl (TIPS) group afforded fuligocandin B (**3**). The <sup>1</sup>H and <sup>13</sup>C NMR spectra of synthetic fuligocandins A (**2**) and B (**3**) were completely identical to those of natural products, which we reported previously.<sup>13</sup> In addition, synthetic **2** and **3** were both dextrorotatory, being consistent with optical rotation data of natural products (**2** and **3**).<sup>13</sup>



**Scheme 1.** Total synthesis of fuligocandin B (**3**). *Reagents and conditions:* (a) PyBOP,  $(i\text{Pr})_2\text{NEt}$ , 96%; (b) LiOH, THF-MeOH-H<sub>2</sub>O; PyBOP,  $(i\text{Pr})_2\text{NEt}$ , 79% (2 steps); (c) LiC≡C-Me, THF, -78 °C, 50%; (d) CF<sub>3</sub>COOH, CH<sub>2</sub>Cl<sub>2</sub>, -20 °C, 90% (70% ee); (e) aldehyde (**10**), LDA, THF, -78 °C to 0 °C; 1M HCl, 63% (2 steps).

Thus, the absolute stereochemistry of C-11a position of both fuligocandins A (**2**) and B (**3**) was revealed as *S*.<sup>19</sup> Since fuligocandin A (**2**) was obtained from fuligocandin C (**4**) through decarboxylation, the absolute stereochemistry of C-11a position of fuligocandin C (**4**) was suggested as *S*, being the same as that of **2**. We also synthesized the enantiomer of fuligocandin B (*ent*-**3**) starting from D-proline, and *ent*-**3** showed levorotation as expected.<sup>20</sup>

We also examined TRAIL resistance-overcoming activity of synthetic compounds using human gastric adenocarcinoma (AGS) cells, which have been used as a model system for evaluating cancer cell apoptosis and are reported to be refractory to apoptosis induction by TRAIL.<sup>21</sup> TRAIL resistance-overcoming activity was assessed by comparing the cell viability of AGS cells on treatment with test compounds in the presence and absence of TRAIL (100 ng/mL),<sup>22</sup> which was evaluated by fluorometric microculture cytotoxicity assay (FMCA).<sup>23</sup> If treatment of AGS cells with a test compound in the presence of TRAIL resulted in decreased cell viability compared with that in the absence of TRAIL, this compound can be considered as an active sample having TRAIL resistance-overcoming activity.

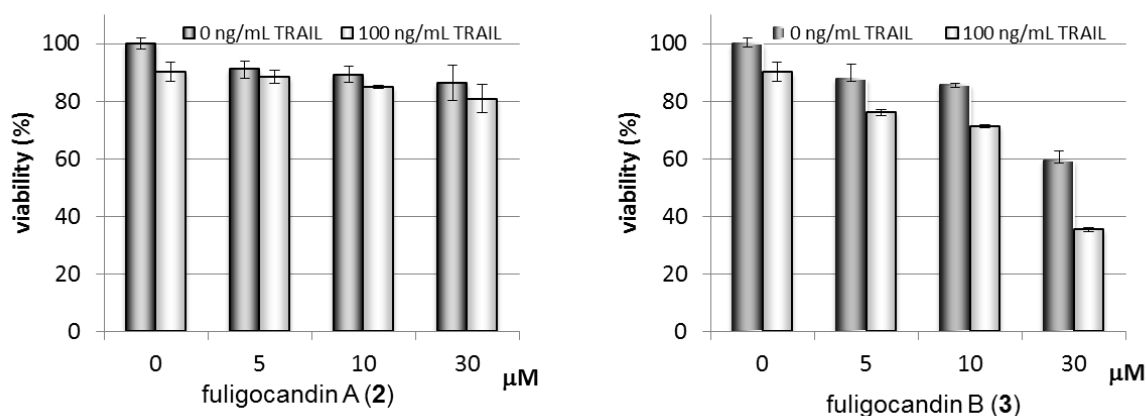


**Figure 3.** Evaluation of TRAIL resistance-overcoming activity of fuligocandins A (2) and B (3).

Combined treatment with TRAIL and synthetic fuligocandin B (3) showed TRAIL resistance-overcoming activity in a dose-dependent manner (Figure 3), while fuligocandin A (2) and *ent*-fuligocandin B (*ent*-3, data not shown) did not show any activity. Further studies on the synthesis of a series of fuligocandin derivatives as well as evaluation of their effects on TRAIL signaling are currently underway in our group.

### 3. PEPTIDE LACTONE DERIVATIVES WITH WNT SIGNAL INHIBITORY ACTIVITY

The fruit bodies of the myxomycete *Physarum melleum* (Figure 4) were collected in Tokorozawa, Saitama Prefecture, Japan. The spores contained in the fruit bodies were subjected to a laboratory culture experiment developed in our group,<sup>24</sup> spreading its spores on an agar medium together with a suspension of *Escherichia coli*. After germination of the spores into myxamoebae, which were visualized by plaque formation in the *E. coli* culture, the myxamoebic plaques were then repetitively transferred to new agar plates several times to remove contaminating organisms. These myxamoebic cultures then proceeded to develop into the plasmodial stage, and these plasmodial cultures (Figure 5) were able to grow by adding oatmeal to the agar medium in the absence of *E. coli*. Finally, the plasmodial culture of *P. melleum* showed the

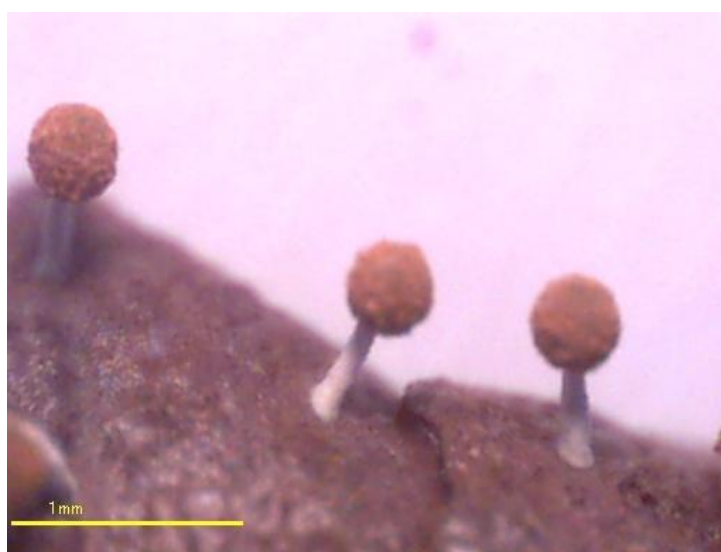


**Figure 4.** Wild fruit body of *Physarum melleum*



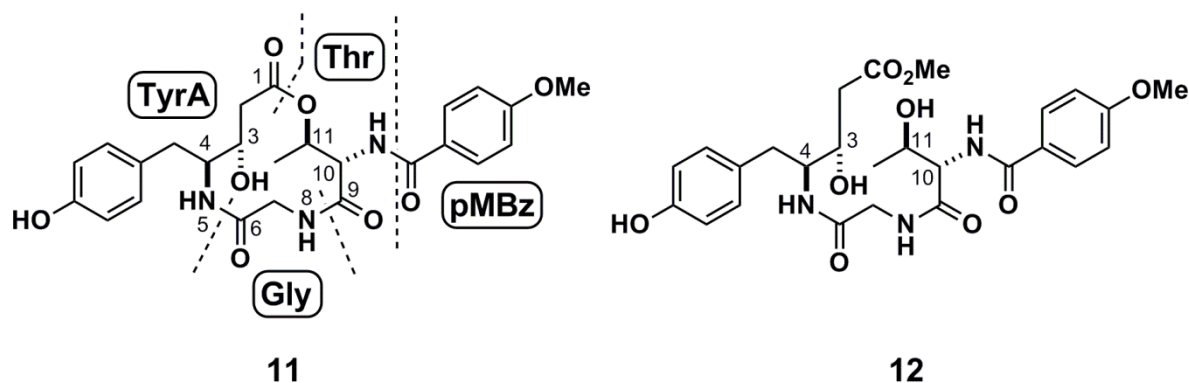
**Figure 5.** Cultured plasmodium of *P. melleum*



**Figure 6.** Cultured fruit body of *P. melleum*

formation of fruit bodies (Figure 6) on the oatmeal agar plates in the presence of light; these results implied that spore-to-spore cultivation, i.e., rotation of one life cycle, was realized on agar plates of *P. melleum*. Spores contained in the cultured fruit bodies were frozen for preservation in a skim milk-glucose suspension and could be used for further spore germination experiments when necessary.

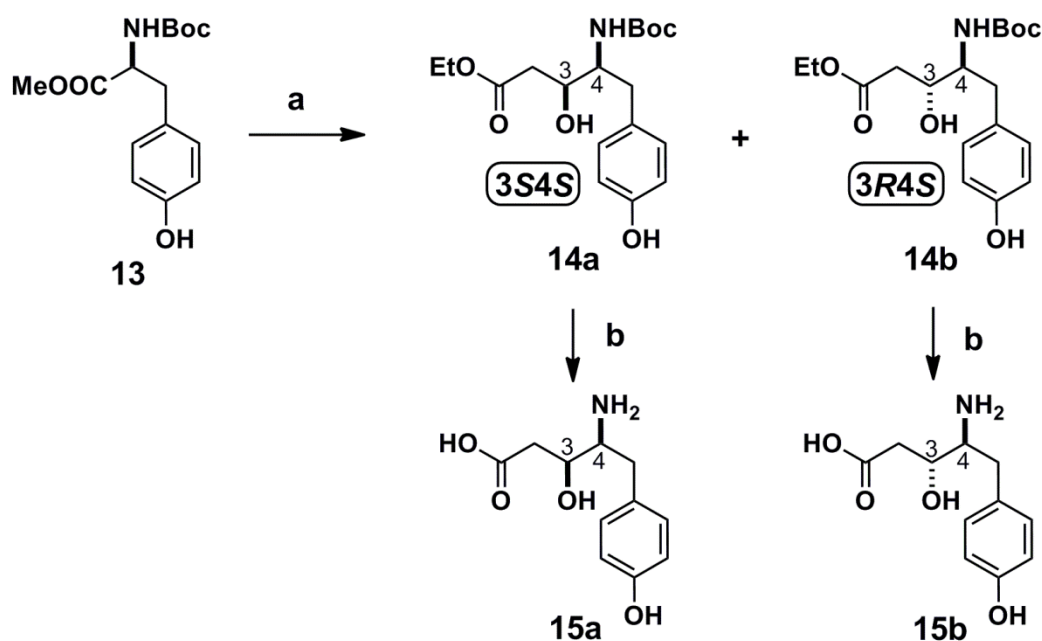
The plasmodium of this myxomycete, *P. melleum*, obtained in a plate culture was mass-cultured in the laboratory on agar plates in the presence of *Escherichia coli*. The harvested plasmodial cells (19.5 g from 2112 plates (9 cm $\phi$ )) were extracted with 90% MeOH and 90% acetone, and the combined extract was partitioned between ethyl acetate and water. The ethyl acetate-soluble layer was subjected to silica gel column chromatography, followed by separation with HPLC on ODS eluted with 50% MeOH to give two UV(254 nm)-positive compounds, named melleumins A (**11**) and B (**12**), in 0.007 and 0.02% yield, respectively.<sup>25</sup>



Spectral studies of these compounds revealed that melleumin A (**11**) was a new peptide-lactone consisting of four units, *p*-methoxybenzoic acid (pMBz), threonine (Thr), glycine (Gly), and an unusual amino acid,

a tyrosine-attached acetic acid (TyrA) and melleumin B (**12**) corresponded to the seco-acid methyl ester of melleumin A (**11**). Treatment of **11** with 28% MeONa afforded **12**, which was detected on the basis of TLC examination. The stereochemistry of the chiral centers at C-3, C-10, and C-11 positions was examined using compound **12**. After acid hydrolysis of **12** (6M HCl, 110 °C, 12 h), the resulting hydrolyzate was subjected to chiral TLC analysis using L-Thr and D-Thr reference samples to reveal that the threonine residue was L (10*S*, 11*R*). In addition, compound **12** was converted to its (*R*)- and (*S*)-MTPA esters, and on the basis of the modified Mosher's method, the absolute configurations of the carbons bearing a secondary hydroxyl group (C-3 and C-11) were revealed as 3*S* and 11*R*. The 11*R* configuration suggested by the modified Mosher's method was consistent with the result from chiral TLC analysis as above.

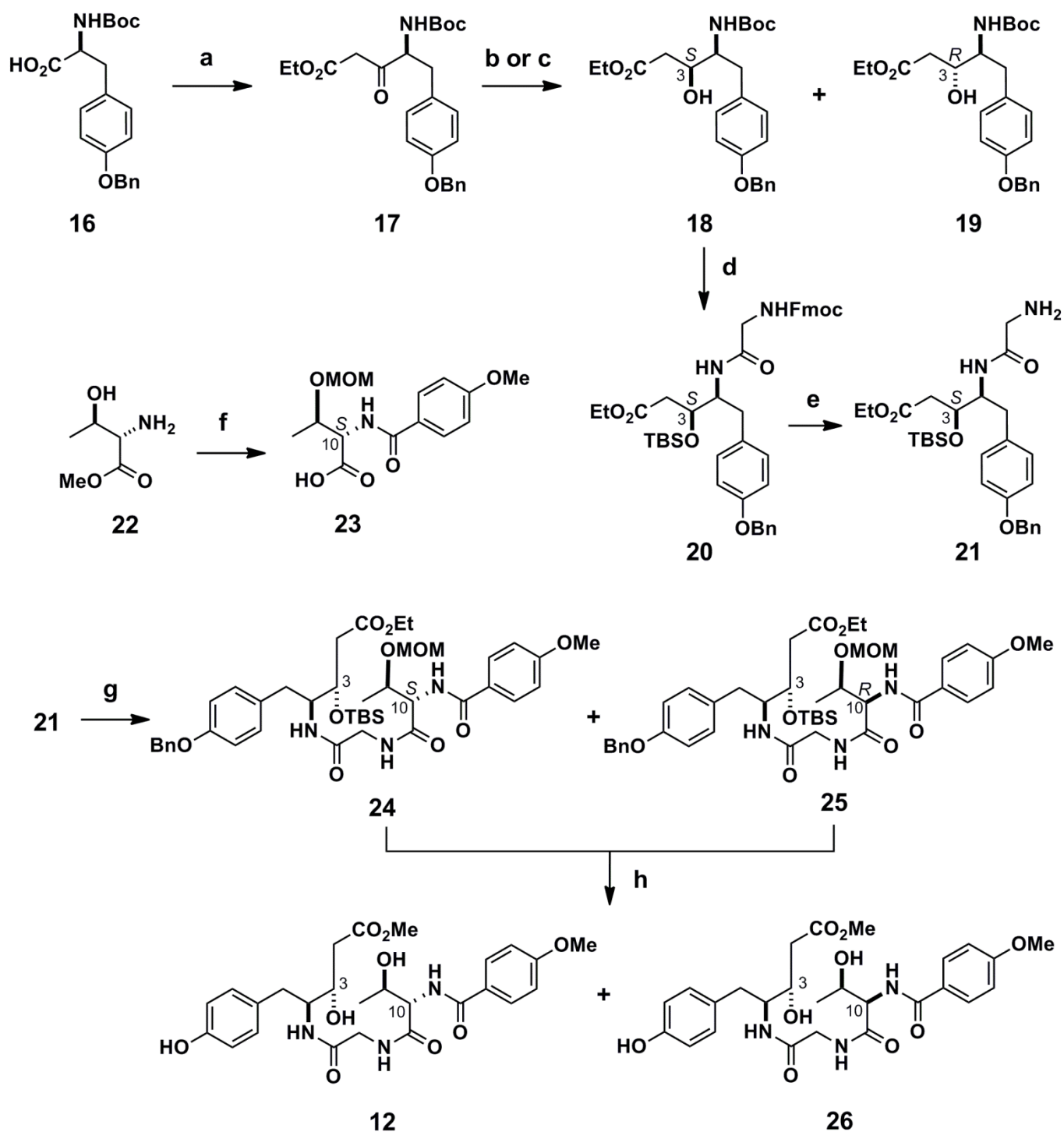
The absolute stereochemistry of the C-4 position, however, remained undefined. To determine the absolute configuration of C-4, which was included in the TyrA unit, we prepared two diastereomers of TyrA by synthesis from L-tyrosine, as shown in Scheme 2. Reduction of the *N*-Boc-L-tyrosine methyl ester (**13**) with DIBAL afforded an aldehyde, which was treated with a lithium enolate of ethyl acetate to give two diastereomers (**14a** and **14b**) in a ratio of 54:46. These diastereomers were separated by silica gel column chromatography and their stereochemistry was assigned on the basis of the Kusumi-Mosher method to have 3*S*4*S* for **14a** and 3*R*4*S* for **14b**, respectively. Deprotection of Boc and ethyl ester groups of **14a** and **14b** was carried out separately by two steps to afford TyrA diastereomers (**15a** and **15b**)



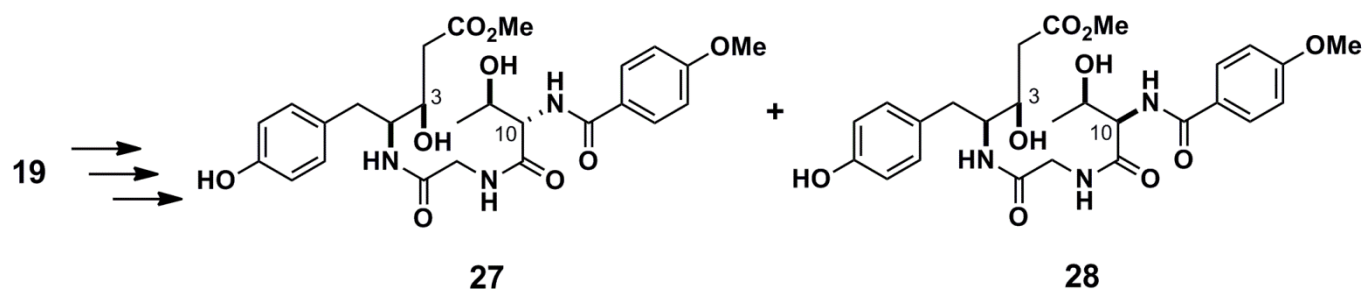
**Scheme 2.** Preparation of TyrA diastereomers. *Reagents and conditions:* (a) 1) DIBAL, toluene; 2) LDA, EtOAc; (b) 1) LiOH, aq. THF-MeOH; 2) TFA, CH<sub>2</sub>Cl<sub>2</sub>.

**15b**), respectively. Comparison of the reversed-phase HPLC retention time between melleumin B (**12**) hydrolysate and the synthetic TyrA units (**15a** and **15b**) showed that the retention time of **15a** matched that of the specimen obtained from **12**. Since melleumin B (**12**) was obtained by treatment of melleumin A (**11**) with 28% MeONa, melleumins A (**11**) and B (**12**) were revealed to have the same stereochemistry. These results suggested that melleumins A (**11**) and B (**12**) had the same stereochemistry as **15a** (3*S*4*S*), and the absolute configurations of 4 chiral centers of **11** and **12** were determined as 3*S*, 4*S*, 10*S*, and 11*R*. We next achieved total synthesis of melleumin B (**12**), as shown in Scheme 3, which provided unequivocal evidence of the whole structure of melleumin B (**12**) and, consequently, that of melleumin A (**11**). *N*-Boc-*O*-benzyl-L-tyrosine (**16**) was treated with carbonyldiimidazole, followed by treatment with a lithium enolate of ethyl acetate to give  $\beta$ -ketoester (**17**). Stereoselective reduction of **17** with K-selectride afforded the desired (3*S*,4*S*)- $\beta$ -hydroxyl ester (**18**) in a ratio of **18**:**19** = 93:7. When sodium borohydride was used in ethanol, (3*R*,4*S*)-TyrA unit (**19**) was predominantly obtained (**18**:**19** = 9:91) and used for the synthesis of 3-*epi*-melleumin B (**27**). For the synthesis of melleumin B (**12**), (3*S*,4*S*)-diastereomer (**18**) was first treated with TBSOTf for deprotection of the Boc group, and then 2,6-lutidine was added to give a free amine, which was subjected to coupling with Fmoc-Gly to give a dipeptide (**20**), and subsequent deprotection of the Fmoc group gave the TyrA-Gly unit (**21**). The L-Thr-pMBz unit (**23**) was prepared from L-threonine methyl ester hydrochloride (**22**) in 3 steps. Coupling of **21** with **23** in the presence of EDC, HOObt, and DMAP afforded tripeptide (**24**) along with its 10*R*-epimer (**25**) through racemization during the coupling reaction (**24**:**25** = 92:8, determined by <sup>1</sup>H NMR). Since the bioactivity of the 10*R*-epimer (**25**) was also interesting, we decided to separate the isomers in the final step. Deprotection of the TBS and MOM groups, followed by hydrolysis of the ethyl ester gave a *seco* acid, which was converted to a methyl ester with trimethylsilyldiazomethane. The benzyl group was finally removed by hydrogenolysis to afford a mixture of melleumin B (**12**) and its 10-epimer (**26**) in a ratio of 91:9, determined by HPLC. Melleumin B (**12**) and its 10-epimer (**26**) were separated as a pure form by reversed-phase HPLC, and the spectral data of synthetic melleumin B (**12**) were completely identical to those of the natural product specimen. Thus, the structure of melleumin B (**12**) as well as melleumin A (**11**) was unambiguously established, including the absolute stereochemistry.<sup>26</sup> Starting from (3*R*,4*S*)-TyrA unit (**19**), 3-*epi*-melleumin B (**27**) and its 10-epimer (**28**, 3-*epi*-10-*epi*-melleumin B) were obtained in a ratio of 83:17, as shown in Scheme 4 by the same procedures as those in Scheme 3.<sup>27</sup>

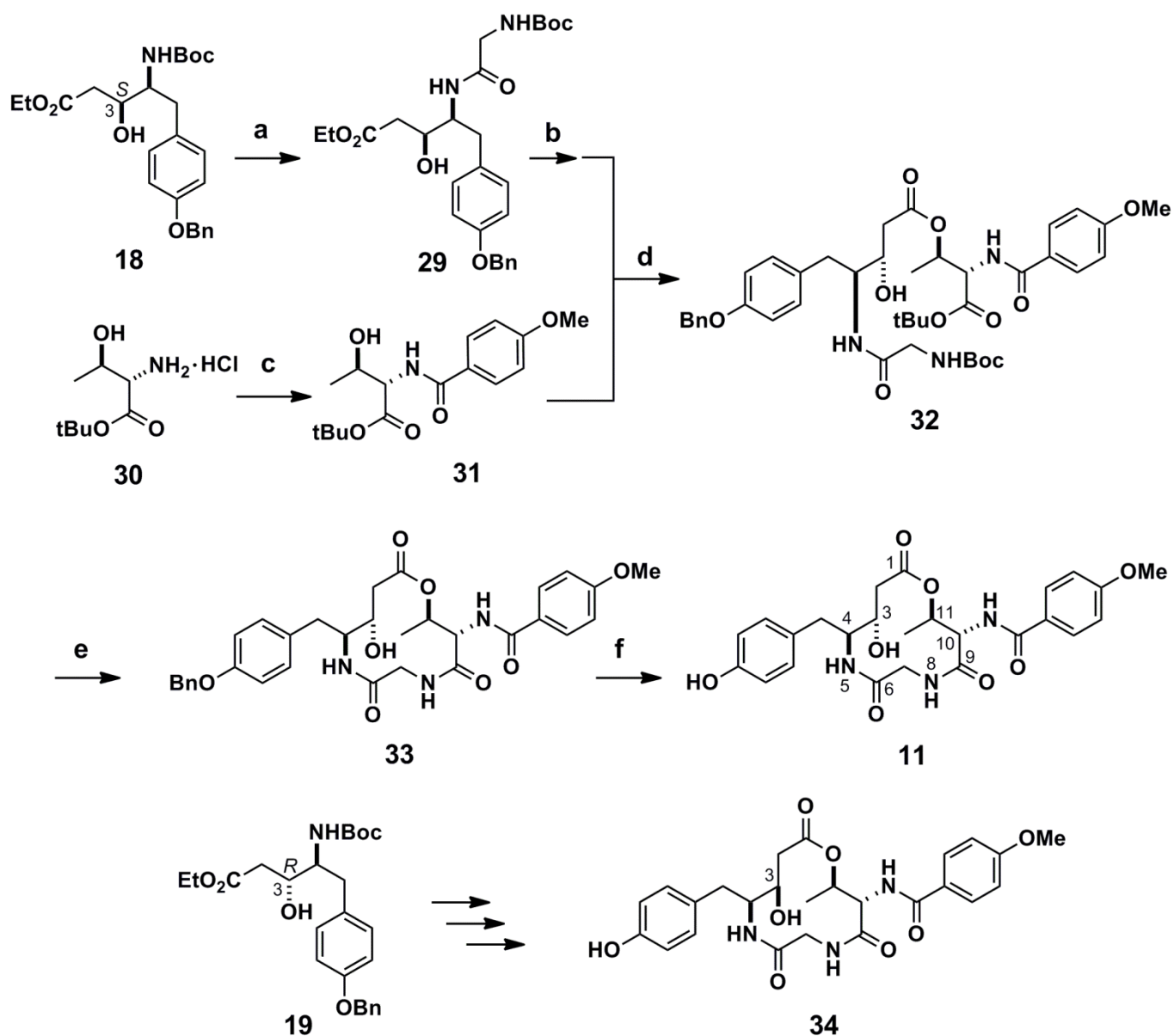
Total synthesis of melleumin A (**11**) was first reported by Luo *et al.* and they also prepared 4*R*-epimer and other derivatives of **11** by intramolecular lactamization at the N5-C6 amide bond.<sup>28</sup> Our first attempt to synthesize melleumin A (**11**) was based on intramolecular lactone formation of the *seco* acid of **11** obtained from hydrolysis of the methyl ester group of synthetic melleumin B (**12**), which was, however,



**Scheme 3.** Total synthesis of melleumin B (**12**) and its 10-epimer (**26**). *Reagents and conditions:* (a) 1) CDI, overnight; 2) EtOAc, LDA, 60% in 2 steps; (b) K-selectride (2.4 eq), THF, 0 °C, 69% (**18:19** = 93:7); (c) NaBH<sub>4</sub> (1.5 eq), EtOH, -78 °C, 94% (**18:19** = 9:91); (d) 1) TBSOTf, then 2,6-lutidine; 2) Fmoc-Gly, EDC, HOBT, DMAP (78% in 2 steps); (e) piperidine; (f) 1) *p*-anisoyl chloride, 66%; 2) MOMCl, 97%; 3) LiOH, 95%; (g) **23**, EDC, HOObt, DMAP, 67% (2 steps from **20**, **24:25** = 92:8); (h) 1) TBAF; 2) HCl, 60 °C; 3) LiOH; 4) TMSCHN<sub>2</sub>; 5) H<sub>2</sub>, 10% Pd/C, 56% (5 steps, **12:26** = 91:9).



**Scheme 4.** Synthesis of 3-*epi*-melleumin B (27) and its 10-epimer (28)



**Scheme 5.** Total synthesis of melleumin A (11). *Reagents and conditions:* (a) 1) TFA; 2) Boc-Gly, EDC, HOBT, DMAP, 80% (2 steps from 18); (b) LiOH, 0 °C; (c) *p*-anisoyl chloride, 99%; (d) 31, DCC, DMAP, 50% (2 steps from 29); (e) 1) TFA; 2) FDPP, 28% (2 steps from 32); (f) H<sub>2</sub>, 10% Pd/C, 97%.

unsuccessful under several conditions. We next examined a strategy based on intramolecular cyclization of the N8-C9 amide bond, as shown in Scheme 5. After deprotection of the Boc group of (3*S*,4*S*)-TyrA unit (**18**) obtained in Scheme 3, coupling of *N*-Boc-glycine gave a dipeptide (**29**) in good yield. Hydrolysis of the ethyl ester of **29**, followed by coupling with the *tert*-butyl ester of pMBz-L-Thr unit (**31**) in the presence of DCC and DMAP, afforded compound **32**. The pMBz-L-Thr unit (**31**) was prepared from L-threonine *tert*-butyl ester hydrochloride (**30**) and *p*-methoxybenzoyl chloride. After deprotection of Boc and the *tert*-butyl group of **32**, macrolactamization in the presence of FDPP gave a cyclic product (**33**). Hydrogenolysis of **33** to remove the benzyl group finally afforded melleumin A (**11**). X-Ray crystallographic analysis of synthetic melleumin A (**11**) was successful, as shown in Figure 7, which provided further corroborating evidence of the total structure of melleumin A (**11**). Starting from (3*R*,4*S*)-TyrA unit (**19**), 3-*epi*-melleumin A (**34**) was obtained as shown in Scheme 5 by the same procedures used for the synthesis of melleumin A (**11**).

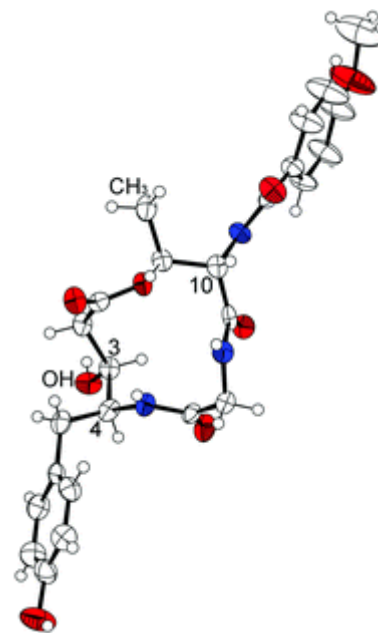
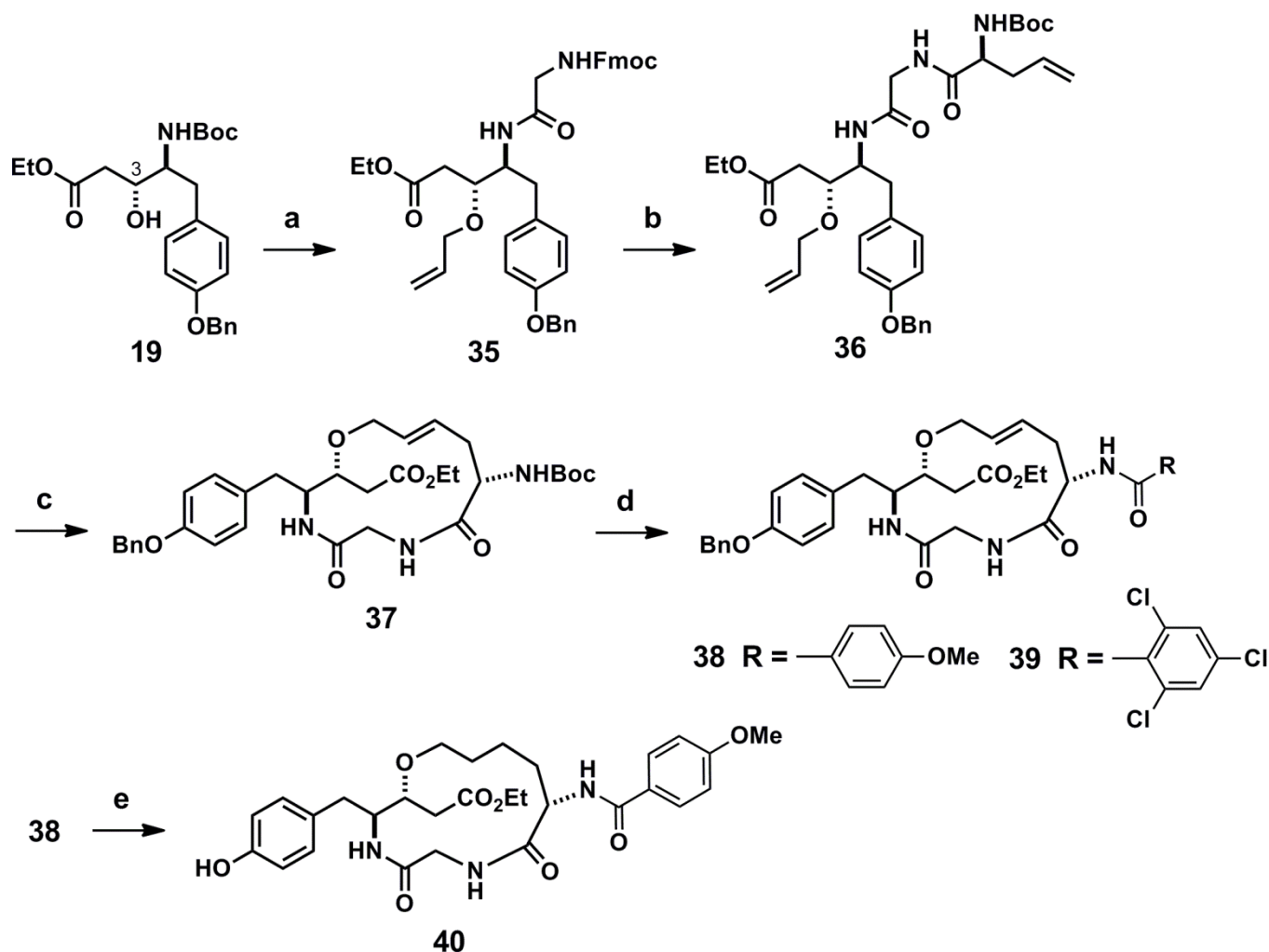


**Figure 7.** X-Ray structure of synthetic melleumin A (**11**)

We also prepared a series of melleumin-like compounds possessing a 13-membered ring without unstable lactone moiety, as shown in Scheme 6. After allylation of the C-3 hydroxyl group of (3*R*,4*S*)-TyrA unit (**19**) by Pd catalyst, deprotection of the Boc group followed by coupling with glycine unit gave **35** in good yield. The coupling reaction with *N*-Boc-L-allylglycine afforded compound **36**, which was subjected to ring-closing metathesis (RCM) reaction with a second-generation Grubbs' catalyst, proceeded smoothly to give a cyclized product with a 13-membered ring (**37**) in 98% yield in 20 min. After removal of the Boc group of **37**, treatment with two acyl chlorides afforded benzamides (**38** and **39**), respectively. Hydrogenation of anisylamide (**38**) afforded a saturated phenol (**40**).<sup>29</sup>

Using these synthetic melleumin-related compounds, we examined Wnt signal inhibitory activity by a luciferase reporter gene assay (Figure 8), as we recently became interested in screening studies targeting this signaling pathway.<sup>30,31</sup> The Wnt signaling pathway regulates many significant biological processes involved in embryogenesis, development, cell polarization, differentiation, cell fate determination, proliferation, and the self-renewal of stem and progenitor cells as well as important functions in adult cells.<sup>32</sup> Aberrant hyperactive or hypoactive signaling of the Wnt pathway is linked to a range of diseases, most notably cancer. Altering Wnt signaling activity therefore may be therapeutic in various clinical



**Scheme 6.** Synthesis of melleumin-like compounds. *Reagents and conditions:* (a) 1) allyl ethyl carbonate, Pd<sub>2</sub>(dba)<sub>3</sub>, dppb, THF, 65 °C, 96%; 2) TFA; 3) Fmoc-glycine, PyBOP, HOBt, DIPEA, 61% (2 steps); (b) 1) piperidine; 2) *N*-Boc-L-allylglycine, PyBOP, HOBt, *i*Pr<sub>2</sub>NEt, 83% (2 steps); (c) 2<sup>nd</sup> Grubbs' cat. (20 mol%), CH<sub>2</sub>Cl<sub>2</sub>, reflux, 98%; (d) 1) TFA; 2) *p*-methoxybenzoylchloride or 2,4,6-trichlorobenzoyl chloride, TEA, 54% for **38** (2 steps) and 53% for **39** (2 steps); (e) H<sub>2</sub>, Pd/C, 70%.

contexts and useful in the development of stem-cell-based therapies. Wnt signaling inhibitors may be suitable for the treatment of not only cancer, but also cardiovascular diseases, schizophrenia, osteoarthritis, tuberous sclerosis, and polycystic kidney disease, while Wnt signaling activators may be useful for degenerative diseases such as tetra-amelia, osteoporosis, familial exudative vitreoretinopathy, tooth agenesis, and Alzheimer disease, as well as the regeneration of tissues and organs. Although, in recent reports, several Wnt signaling inhibitors have been identified,<sup>33,34</sup> further studies of small molecules that not only inhibit but also augment Wnt signaling will be of great importance given their broad potential applications.<sup>35</sup>

Wnt signaling activates gene transcription with a complex between  $\beta$ -catenin and TCF/LEF, which is a DNA-binding protein. SuperTOP-Flash (Prof. R. T. Moon, University of Washington), a reporter plasmid with multiple TCF-binding sites (CCTTTGATC), was stably transfected into 293 cells (Prof. J. Nathans, Johns Hopkins Medical School). SuperFOP-flash has eight mutated TCF-binding sites (CCTTTGGCC); therefore, a selective inhibitor would not show enhanced transcription in SuperFOP-Flash-transfected cells; thus, these cells provide a negative control for the assay and the TOP/FOP-Flash reporter activation ratio provides a measure of the selectivity of Wnt signal inhibition. It is also possible that the decrease of luciferase reporter activity in this assay was due to the cytotoxicity of the test samples. We therefore also examined the cytotoxicity of samples using a fluorimetric microculture cytotoxicity assay (FMCA).<sup>23</sup> Compounds exhibiting both low luciferase reporter activity and high cell viability were suitable for our purpose.

Melleumin A (**11**) showed weak inhibitory activity and 3-*epi*-melleumin A (**34**) was inactive, while melleumin B (**12**) and its epimers (**26–28**) as well as melleumin-related 13-membered ring compounds (**38–40**) all exhibited moderate inhibitory activity (Figure 8). Figure 9 shows Wnt signal inhibitory activity of melleumin A (**11**) and a 13-membered ring compound (**38**) with different concentrations along with their cell viability. Melleumin A (**11**) and melleumin B (**12**) reduced Wnt transcriptional activity to 74% and 64%, respectively. Of them, 10-*epi*-melleumin B (**26**) proved to be the most active (46%). Among synthetic cyclic melleumin-like compounds, anisylamide benzyl ether (**38**) showed 20% more inhibition (54%) than melleumin A (**11**) with high cell viability (Figures 8 and 9).

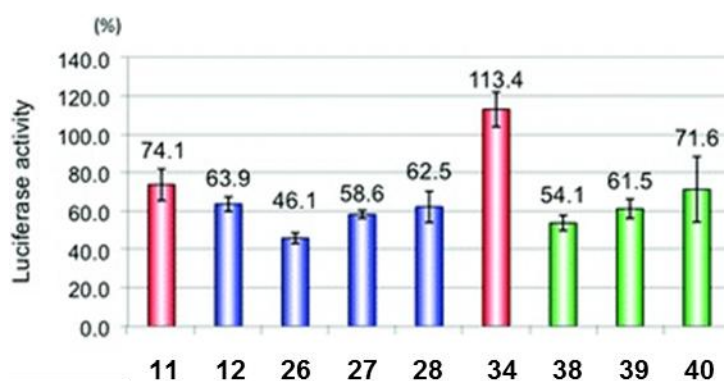


**Figure 8.** Comparison of Wnt signal inhibition activity of melleumin-related compounds at 50  $\mu$ M. Fold activation of Super TOP-Flash (solid columns). STF/293 cells (a 293 human embryonic kidney cell line stably transfected with Super Top-Flash,  $3 \times 10^4$ ) were split into 96-well plates and 24h later cells were treated with 15 mM LiCl and testing samples (DMSO solution).  $N = 3$ , Bars = sd. The activity of the untreated cells was defined as 100%.

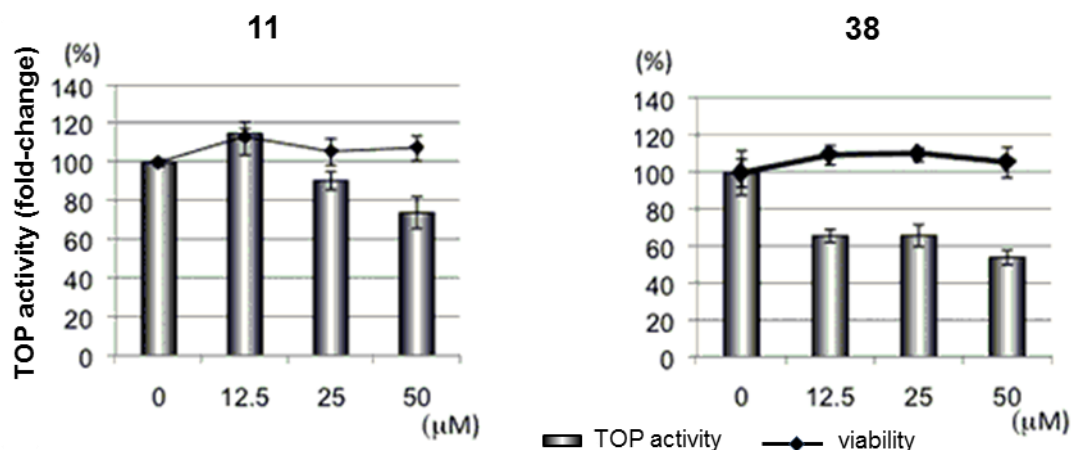


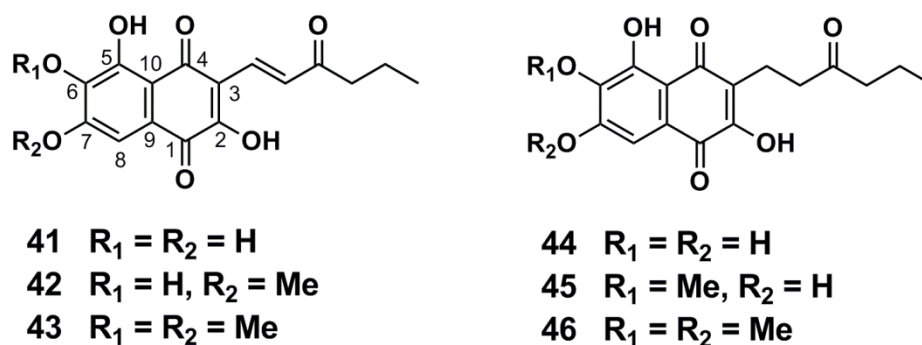
**Figure 9.** Wnt signal inhibition activity of melleumin-related compounds. Fold activation of Super TOP-Flash (solid columns) and cell viability (solid curves). STF/293 cells ( $3 \times 10^4$ ) were split into 96-well plates and, 24h later, cells were treated with 15 mM LiCl and testing samples (DMSO solution). Super FOP-Flash activities at each concentration were not affected (data not shown).  $N = 3$ , Bars = sd.

#### 4. NAPHTHOQUINONE PIGMENT WITH HES1 DIMERIZATION INHIBITION ACTIVITY

The fruit bodies of the myxomycete *Lindbladia tubulina* (Figure 10), collected at Takamagahara, Kochi, Japan, were extracted with MeOH, and the MeOH extract was partitioned between EtOAc and water. The water-soluble fraction, which was suggested to contain red pigments by TLC examinations, was subjected to chromatography on ODS and Sephadex LH-20, followed by further purification with HPLC on ODS to give three naphthoquinone pigments, lindbladione (**41**), 7-methoxylindbladione (**42**), and 6,7-dimethoxylindbladione (**43**). The EtOAc-soluble fraction was also subjected to chromatography on silica gel and Sephadex LH-20 to afford three different naphthoquinone pigments, dihydrolindbladione (**44**), 6-methoxydihydrolindbladione (**45**), and 6,7-dimethoxydihydrolindbladione (**46**). Although the compound name and structure of lindbladione (**41**) were found in a symposium proceeding by Steglich's group,<sup>36</sup> no experimental details or the spectral data of **41** have been reported in the literature. We therefore described for the first time full



**Figure 10.** Wild fruit bodies of *Lindbladia tubulina*



characterization of compound **41** and the isolation and structure elucidation of other five new compounds (**42–46**).<sup>37,38</sup>

A high throughput screening system for small molecule inhibitors of the basic helix-loop-helix (bHLH) transcriptional repressor factor Hes1 was constructed in our laboratory.<sup>39</sup> The bHLH repressor and activator genes play an essential role in embryogenesis, neurogenesis, and the development of many organs.<sup>40</sup> Hes factors (Hes1, Hes3, and Hes5) regulate cell proliferation and differentiation in the nervous system, acting as bHLH repressors through the formation of homo- or heterodimers. bHLH

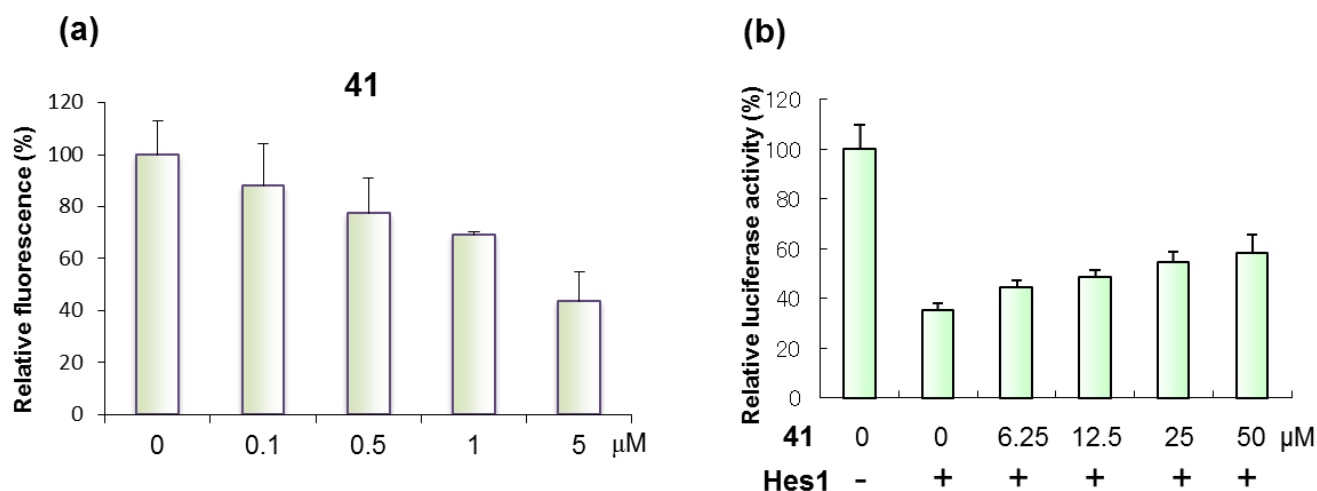


**Figure 11.** Hes1 inhibition activity of lindbladione (**41**). (a) Evaluation of the inhibitory activity of **41** on Hes1 dimer formation on a microplate. Experiments were performed on a microplate containing immobilized Hes1. Excitation was 530 nm and emission was 590 nm. The background value (without Hes1) was subtracted and fluorescence intensity of the blank (DMSO) was normalized to 100%. (b) Inhibitory effect of **41** on Hes1-dependent gene repression in mouse C3H10T1/2 cells transfected with pN6- $\beta$ A-luc, pCL-Hes1, and pRL-SV40 in a 24-well plate. Compound was added to the medium 3 h after transfection. After 24 h, luciferase activity was determined. The mean and SD of three individual wells were calculated.

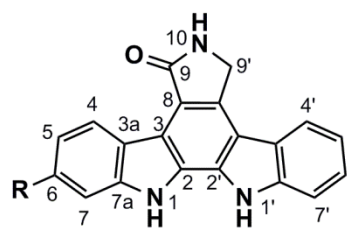
activators such as Mash1 and E47 are suppressed by Hes1 homodimers, and we focused on the inhibition of Hes1 dimer formation, which results in acceleration of bHLH activator transcription and may promote differentiation of neural stem cells (NSCs) into neurons. Small molecules that modulate Hes1 activity are potentially important chemical tools and candidate medicines for neural diseases. We recently developed a rapid in vitro high throughput screening system for identifying Hes1 inhibitors using fluorophore-labeled Hes1 and Hes1 immobilized on microplates. An inhibitor compound which reduces the level of Hes1 dimerization may be detected by a reduction in fluorescence. By this screening system using natural products collection in our laboratory, lindbladione (**41**) was identified as the first Hes1 dimer inhibitor with an  $IC_{50}$  value of 4.1  $\mu$ M (Figure 11a). We subsequently examined the intracellular inhibition activity of **41** by a cell-based reporter assay for measuring the effect on Hes1-induced repression in C3H10T1/2 cells. Decrease of luciferase activity to 35% in the reporter assay was observed in the presence of Hes1, since Hes1 suppresses the transcription of bHLH activators through homodimerization. Compound **41**, having an inhibition effect of Hes1 dimerization, showed dose-dependent inhibition of the Hes1-mediated suppression of gene expression; transcriptional activity assessed by the reporter luciferase activity was recovered by compound **41** to around 60% at 50  $\mu$ M (Figure 11b).

## 5. BISINDOLE ALKALOIDS WITH HEDGEHOG SIGNAL INHIBITORY ACTIVITY

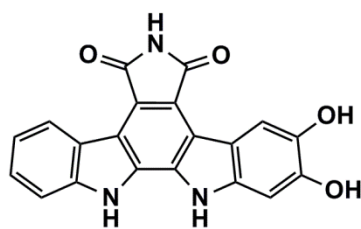
The fruit bodies of the myxomycete *Lycogala epidendrum* (Figure 12), collected in Ohtsu, Kochi, Japan, in 2004, were extracted with 90% MeOH and 90% acetone successively, and the combined crude extract was partitioned between EtOAc and water. The EtOAc-soluble fraction was subjected to silica gel, ODS, and Sephadex LH-20 column chromatography, followed by further purification with reversed-phase HPLC to give two new bisindole alkaloids, 6-hydroxystaurosporinone (**47**) and 5,6-dihydroxyarcyriaflavin A (**48**),<sup>41</sup> along with eight known compounds, which were identified as lycogarubins A–C (**49–51**),<sup>42</sup> lycogamic acid (**52**),<sup>43</sup> arcyriarubin A (**53**),<sup>43</sup> arcyriaflavins A (**54**) and B (**55**),<sup>43</sup> and staurosporinone (**56**).<sup>44</sup> We also isolated three new bisindole alkaloids (**57–**



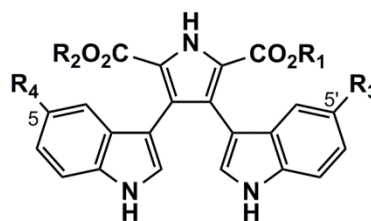
Figure 12. Wild fruit bodies of *Lycogala epidendrum*



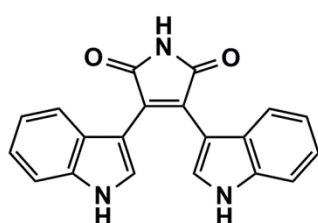
**47** R = OH  
**56** R = H



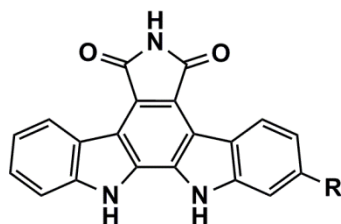
**48**



**49** R<sub>1</sub> = R<sub>2</sub> = Me, R<sub>3</sub> = OH, R<sub>4</sub> = OH  
**50** R<sub>1</sub> = R<sub>2</sub> = Me, R<sub>3</sub> = OH, R<sub>4</sub> = H  
**51** R<sub>1</sub> = R<sub>2</sub> = Me, R<sub>3</sub> = R<sub>4</sub> = H  
**52** R<sub>1</sub> = R<sub>2</sub> = H, R<sub>3</sub> = R<sub>4</sub> = H  
**57** R<sub>1</sub> = Me, R<sub>2</sub> = H, R<sub>3</sub> = R<sub>4</sub> = H  
**58** R<sub>1</sub> = Me, R<sub>2</sub> = H, R<sub>3</sub> = OH, R<sub>4</sub> = H  
**59** R<sub>1</sub> = Me, R<sub>2</sub> = H, R<sub>3</sub> = H, R<sub>4</sub> = OH



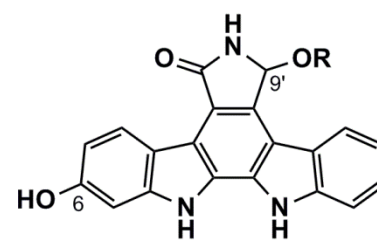
**53**



**54** R = H  
**55** R = OH

**59**), corresponding to monodemethyl derivatives of lycogarubun B (**50**) or C (**51**) from a different collection of *L. epidendrum*.<sup>45</sup>

The fruit bodies of the myxomycete *Perichaena chrysosperma* (Figure 13), collected in Nasu, Tochigi, Japan, in 2009, were extracted with 90% MeOH and 90% acetone successively, and the combined crude extracts were subjected to silica gel and ODS column chromatography to afford a new bisindole alkaloid, 6-hydroxy-9'-methoxystaurosporinone (**60**), together with two known alkaloids, which were identified as 6-hydroxystaurosporinone (**47**) and arcyriflavin B (**55**).



**60** R = Me  
**61** R = H



**Figure 13.** Fruit bodies of *Perichaena chrysosperma*

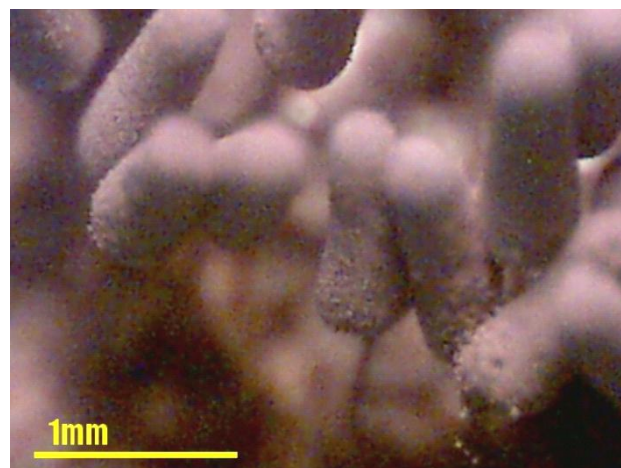


**Figure 14.** Fruit bodies of *Arcyria cinerea*

A related new bisindole alkaloid, 6,9'-dihydroxystaurosporinone (**61**), was also isolated from fruit bodies of *Arcyria cinerea* (Figure 14), collected in Kochi, Japan, in 2004.<sup>46</sup>

During our search for bioactive natural products targeting signaling molecules related to diseases or basic biological processes, we recently found that some of these bisindole alkaloids exhibited hedgehog signal inhibitory activity.<sup>47</sup> The hedgehog (Hh) signaling pathway has been implicated in a variety of developmental processes of differentiation and proliferation in a wide range of organisms, and controls tissue polarity, patterning maintenance, and stem-cell maintenance during embryonic development, while hyperactivation of this pathway has been recognized to cause tumorigenesis in a wide variety of tissues, and Hh signaling may also have a key role in epithelial-to-mesenchymal transition (EMT) and metastases in cancer cells.<sup>48</sup> Thus, small molecules having effects on Hh signaling are anticipated as an effective therapeutic strategy for cancers and other diseases.

For a screening study of Hh signal inhibitors from natural products, we have constructed a cell-based assay system for GLI-mediated transcriptional activity. This is an assay using a transcriptional factor GLI-dependent luciferase reporter in human keratinocyte cells (HaCaT) expressing GLI1 under tetracyclic control (Prof. F. Aberger, University of Salzburg). The 12 consecutive GLI-binding sites (12 x GACCACCCA) and the TK promoter (Prof. R. Toftgård, Karolinska Institute) were inserted into the pGL4.20 plasmid (Promega). The constructed plasmid was stably transfected into HaCaT cells expressing exogenous GLI1 protein under tetracycline control. Using this cell-based assay (HaCaT-GLI1-Luc cells), we identified bisindole alkaloids such as 6-hydroxystaurosporinone (**47**), 5,6-dihydroxyarcyriaflavin A (**48**), and staurosporinone (**56**) as GLI1-mediated transcriptional inhibitors with IC<sub>50</sub> values of 1.8, 3.6, and 6.9 μM, respectively. We confirmed the effect of staurosporinone (**56**) on Hh/GLI signaling component expression in PANC1 cells by semiquantitative RT-PCR analysis. PANC1 cells are a human pancreatic cancer cell line that expresses numerous Hh signaling pathway components, including Shh, Ptch, suppressor of fused, GLI1, and GLI2, indicating that the Hh/GLI signaling pathway is activated in this cell. Staurosporinone (**56**) decreased the mRNA expression of *Gli1*, *Gli2*, and *Ptch* genes, suggesting that this compound inhibited the expression of these components at the transcriptional level. Staurosporinone (**56**) was cytotoxic against PANC1 cells with an IC<sub>50</sub> value of 40.8 μM, while the cytotoxicity of **56** against a mesenchymal progenitor (C3HT10T1/2) cell line derived from the mouse embryonic mesoderm, which is Hh responsive but not reliant on Hh for survival, was 3.3-fold lower (IC<sub>50</sub> value of 137 μM). The hedgehog signal inhibitory activity of 6-hydroxy-9'-methoxystaurosporinone (**60**) was also examined by the luciferase assay system using HaCaT-GLI1-Luc cells to reveal that compound **60** dose-dependently inhibited GLI-mediated transcriptional activity with an IC<sub>50</sub> value of 4.6 μM with high cell viability (Figure 15). Compound **60** was evaluated for cytotoxicity against a panel of cells with increased Hh signaling levels (PANC1 and

DU145) and without reliance on Hh ligand for survival (C3H10T1/2). DU145 cells are a human prostate cancer cell line that also highly expresses Hh signaling pathway components. As a result, compound **60** was shown to be cytotoxic against PANC1 and DU145 ( $IC_{50}$  5.0 and 4.2  $\mu$ M, respectively), but did not affect C3H10T1/2 cells ( $IC_{50}$  >14.0  $\mu$ M; Figure 16).

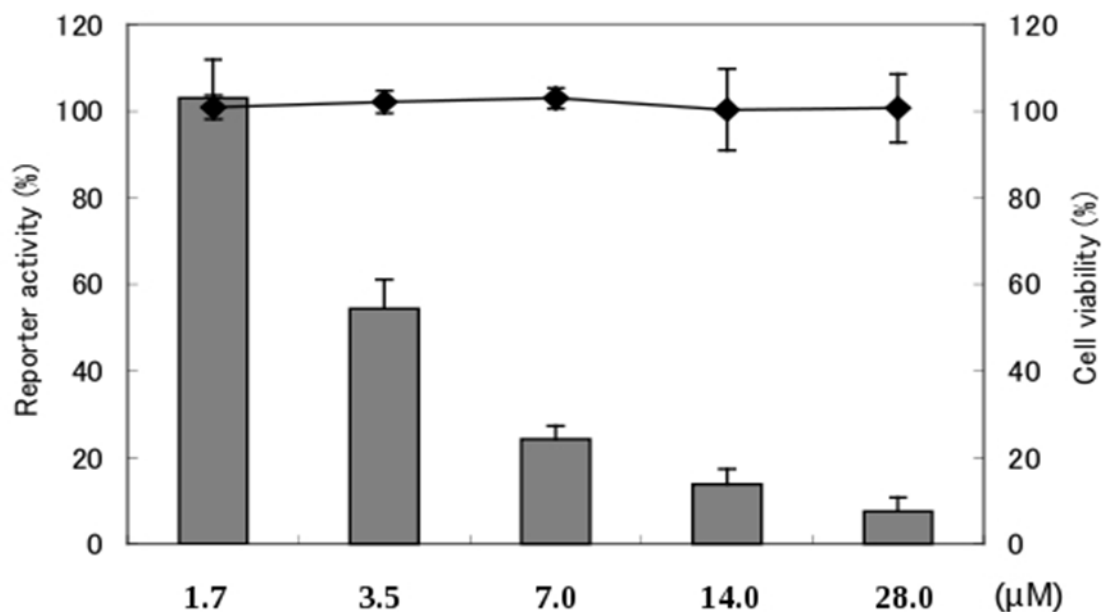


**Figure 15.** Inhibition of GLI1-mediated transcriptional activity (solid columns) and cell viability (solid curves) of compound **60**. HaCaT-GLI1-Luc cells were seeded onto a 96-well plate ( $2 \times 10^5$  cells per well) then treated with compounds after 12 h tetracycline addition. Cell viability and luciferase activity were determined at the same time. The assays were performed at 0.05% DMSO ( $n=3$ ). Error bars represent s.d.

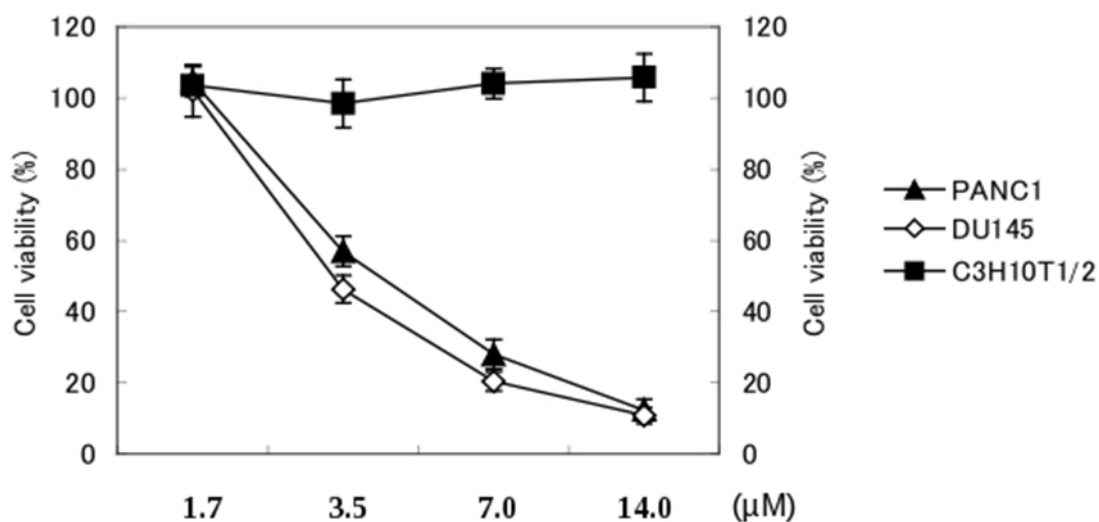


**Figure 16.** Cytotoxicity of compound **60** against PANC1, DU145, and C3H10T1/2 cells. The assays were performed at 0.05% DMSO ( $n=3$ ). Error bars represent s.d.

## 6. BISINDOLE ALKALOIDS WITH WNT OR HES1 INHIBITORY ACTIVITY

The fruit bodies of *Arcyria ferruginea* (Figure 17), collected in Hao, Yasu-cho, Kochi Prefecture, Japan, in 2001, were extracted with 90% MeOH and 90% acetone successively, and the combined crude extracts were subjected to silica gel and Sephadex LH20 column chromatography to afford a new bisindole alkaloid, dihydroarcyriarubin C (**62**) together with two known alkaloids, arcyriarubin C (**63**) and arcyriaflavin C (**64**).<sup>49</sup> Since the stereochemistry of dihydroarcyriarubin C (**62**) remained undetermined, we investigated the synthesis of *cis*- and *trans*-isomers of dihydroarcyriarubin C (**62a** and **62b**, respectively).<sup>50</sup>

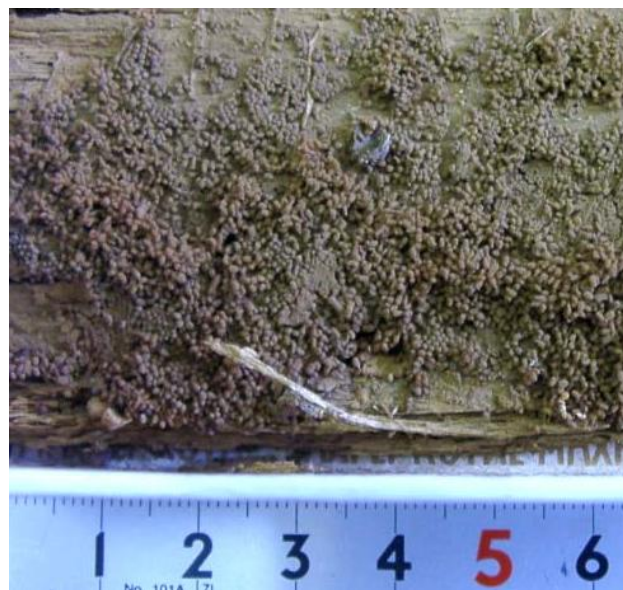
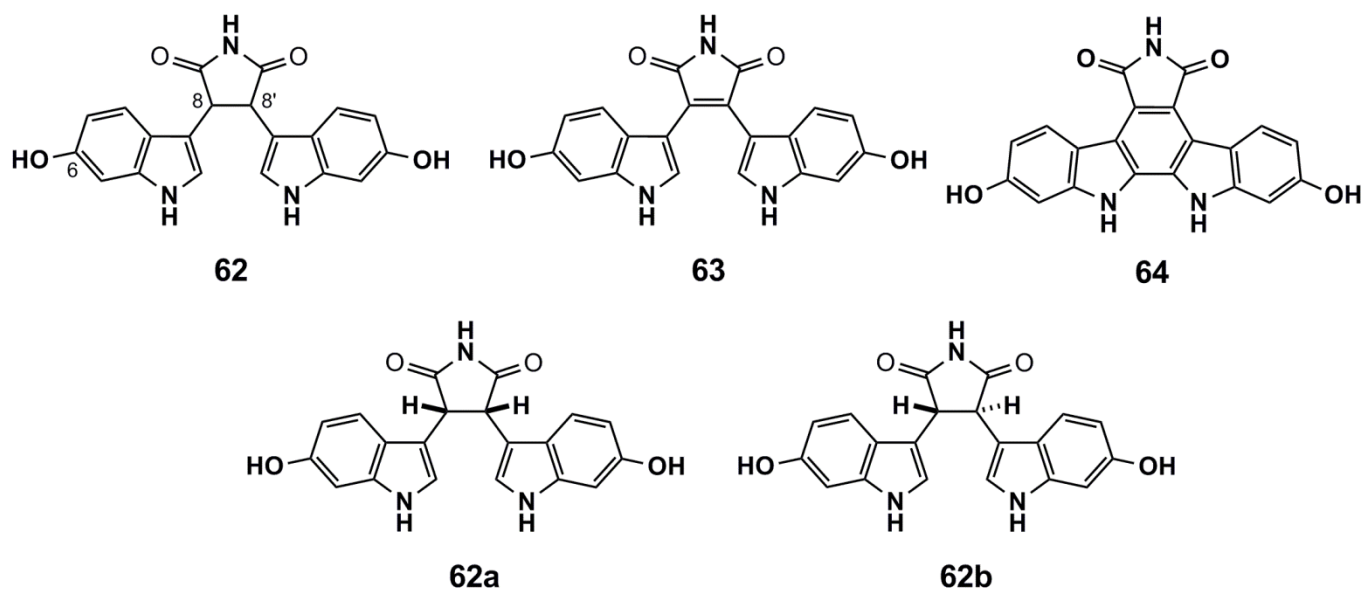
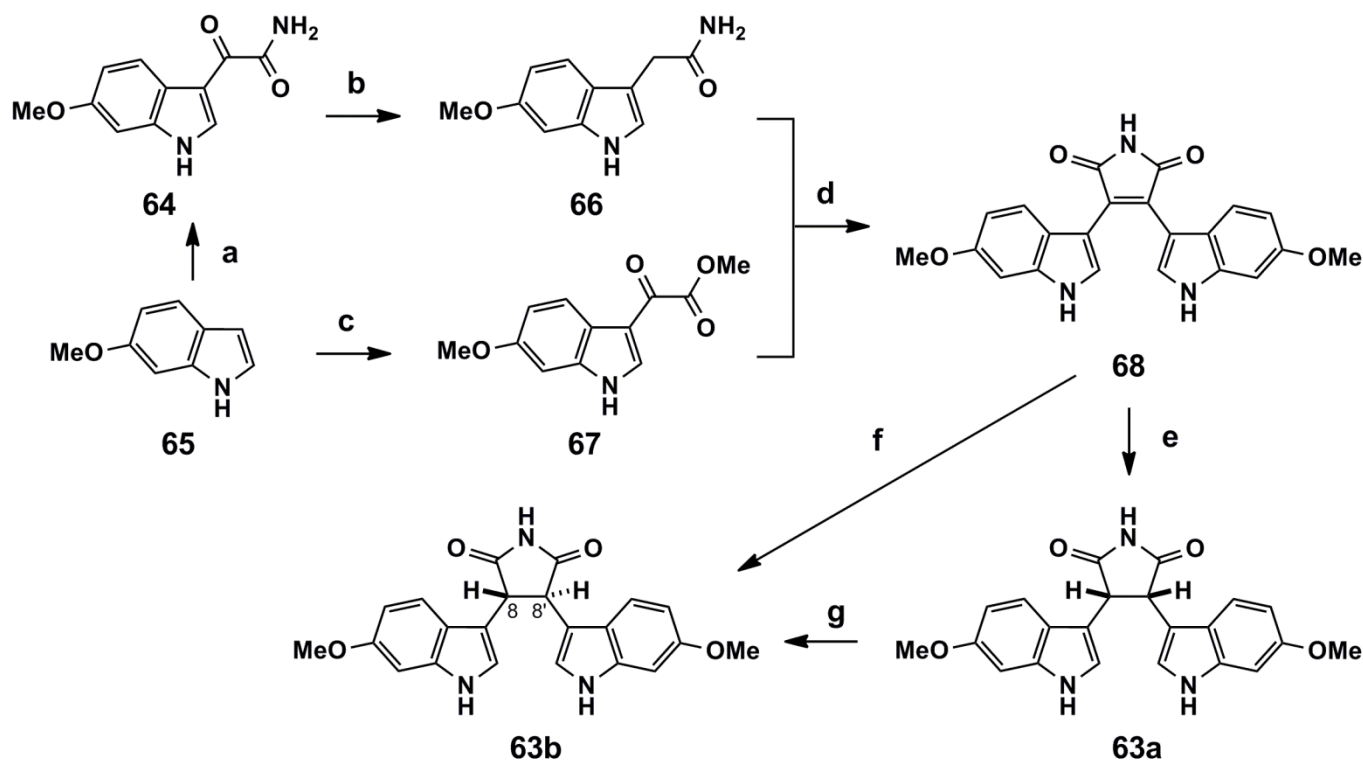


Figure 17. Fruit bodies of *Arcyria ferruginea*

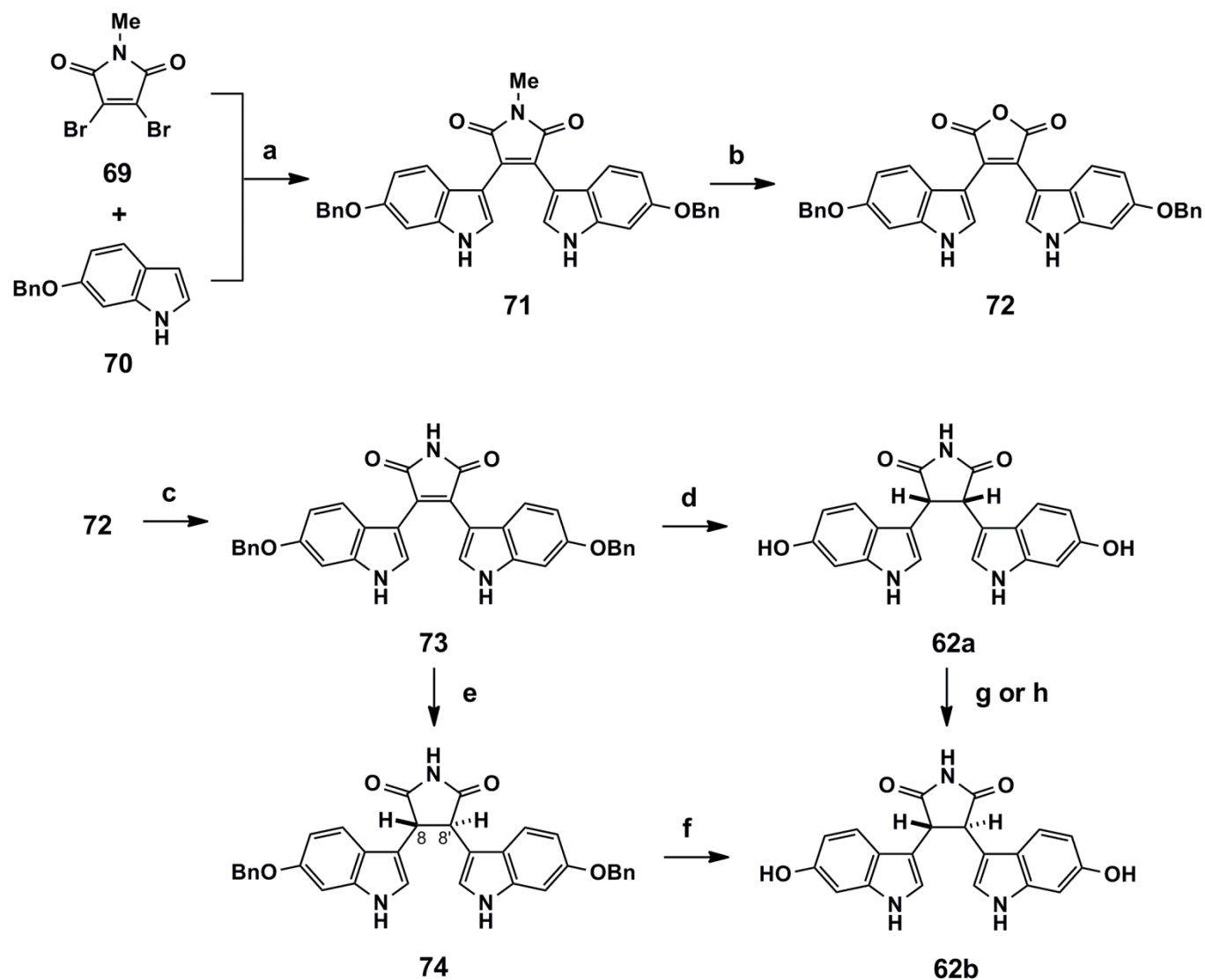


We first studied the synthesis of *cis*- and *trans*-isomers of di-*O*-methyldihydroarcyriarubin C (**63a** and **63b**, respectively), as shown in Scheme 7. Reduction of 6-methoxyindolylglyoxylamide (**64**), prepared from 6-methoxyindole (**65**), with NaBH<sub>4</sub> followed by dehydroxylation under TMSCl and NaI conditions, gave methyl indolylacetamide (**66**). Methyl indolylglyoxlate (**67**), also prepared from **65**, reacted with **66** to give bis-indolylmaleimide (**68**). Hydrogenation with palladium on carbon in methanol afforded 82% yield of the *meso* succinimide (**63a**). The *dl* isomer (**63b**) was readily prepared by treatment of **68** or **63a** with magnesium in refluxing methanol. The <sup>1</sup>H NMR spectra of **63a** and **63b** were compared with



**Scheme 7.** Synthesis of di-*O*-methyldihydroarcyriarubin C isomers. *Reagents and conditions:* (a) 1) (COCl)<sub>2</sub>, THF, -5 °C; 2) aq. NH<sub>3</sub>, 90% (2 steps); (b) 1) NaBH<sub>4</sub>, MeOH, 61%; 2) TMSCl, NaI, MeCN, 0 °C, 35%; (c) 1) (COCl)<sub>2</sub>, THF, -5 °C; 2) MeOH, 68% (2 steps); (d) KO<sup>t</sup>Bu, THF, 0 °C to rt, 50%; (e) H<sub>2</sub>, cat. Pd/C, MeOH, 82%; (f) Mg, MeOH, reflux, 56%; (g) Mg, MeOH, reflux, 57%.

that of natural product **62**, particularly the <sup>1</sup>H NMR chemical shifts of H-8 and H-8' in acetone-*d*<sub>6</sub> [**62** (natural): δ 4.44; **63a** (*cis*): δ 4.94; **63b** (*trans*): δ 4.49] suggesting that **62** has a *trans* configuration. Several methods for deprotecting the *O*-methyl groups of the isomers were examined, but the corresponding bisindole products were not obtained. To change the protective group and improve the yield of the coupling reaction of **66** and **67**, an alternative synthetic route was applied to use the reaction of 2,3-dibromo-*N*-methylmaleimide (**69**) and 4-benzyloxyindole (**70**), followed by the four-step procedure described by Ohkubo *et al.*<sup>51</sup> to give an *N*-methylmaleimide (**71**), as shown in Scheme 8. Compound **71** was converted into a maleic anhydride (**72**) under alkaline conditions in aqueous ethanol. After ammonolysis of **72**, hydrogenation of the maleimide (**73**) afforded the *cis*-isomer (**62a**) through simultaneous deprotection of benzyl groups. Treatment of **73** with Mg gave compound **74** in 84% yield, and then hydrogenolysis of the benzyl group afforded a product **62b**, which was also obtained by epimerization of **62a** under basic conditions and proved to be a thermally stable *trans*-isomer.



**Scheme 8.** Synthesis of dihydroarcyriarubin C isomers. *Reagents and conditions:* (a) 1) LiHMDS, THF,  $-20\text{ }^{\circ}\text{C}$ , 93%; 2)  $(\text{Boc})_2\text{O}$ , DMAP, THF, 90%; 3) **70**, LiHMDS, THF,  $-20\text{ }^{\circ}\text{C}$ , 90%; 4) 40%  $\text{MeNH}_2\text{-MeOH}$ , 81%; (b) KOH (1.0 eq), EtOH/ $\text{H}_2\text{O}$  (5:1), reflux, 89%; (c)  $\text{NH}_4\text{OAc}$ ,  $140\text{ }^{\circ}\text{C}$ , 97%; (d)  $\text{H}_2$ , cat. Pd/C, EtOH, 95%; (e) Mg, MeOH, reflux, 84%; (f)  $\text{H}_2$ , cat. Pd/C, EtOH, 98%; (g) Mg, MeOH, reflux, 81%; (h) DBU, THF, rt to reflux, 93%.

Comparison of the  $^1\text{H}$  and  $^{13}\text{C}$  NMR data of the natural isolated dihydroarcyriarubin C (**62**) and the synthesized *cis*- (**62a**) and *trans*-isomers (**62b**) in acetone- $d_6$  revealed that the chemical shifts of **62b** were identical to those of **62**; the *cis*- and *trans*-isomers were obviously different from each other [H-8 and H-8': **62** (natural):  $\delta_{\text{H}}$  4.44; **62a** (synthetic, *cis*):  $\delta_{\text{H}}$  4.90; **62b** (synthetic, *trans*):  $\delta_{\text{H}}$  4.45; C-8 and C-8': **62** (natural):  $\delta_{\text{C}}$  48.8; **62a** (synthetic, *cis*):  $\delta_{\text{C}}$  46.3; **62b** (synthetic, *trans*):  $\delta_{\text{C}}$  48.9]. Thus, the stereochemistry of dihydroarcyriarubin C (**62**) was revealed to be *trans*.<sup>49</sup> Natural dihydroarcyriarubin

C (**62**) was suggested to be racemic, since its CD spectrum showed an almost negligible curve.

We examined the Wnt signal inhibitory activity of these bisindole alkaloids using a luciferase reporter gene assay (*vide supra*). As a result, the *cis*-isomer (**62a**) of dihydroarcyriarubin C exhibited moderate dose-dependent Wnt signal inhibition activity with high cell viability, whereas *trans*-isomer (**62b**), which is identical to natural product **62**, had almost no effect (Figure 18). Two bisindole alkaloids, lycogarubins B (**50**) and C (**51**) having a pentacyclic nucleus with a pyrrole dicarboxylic acid methyl ester moiety, which were isolated from *Lycogala epidendrum*,<sup>41</sup> showed relatively strong Wnt signal inhibitory activity (Figure 19). On the other hand, arcyriaflavin C (**64**) having a pentacyclic framework with a carbon-carbon bond between C-2 and C-2' position, which was isolated from *Arcyria ferruginea*, did not show significant Wnt signal inhibition activity (Figure 20a), while **64** substantially

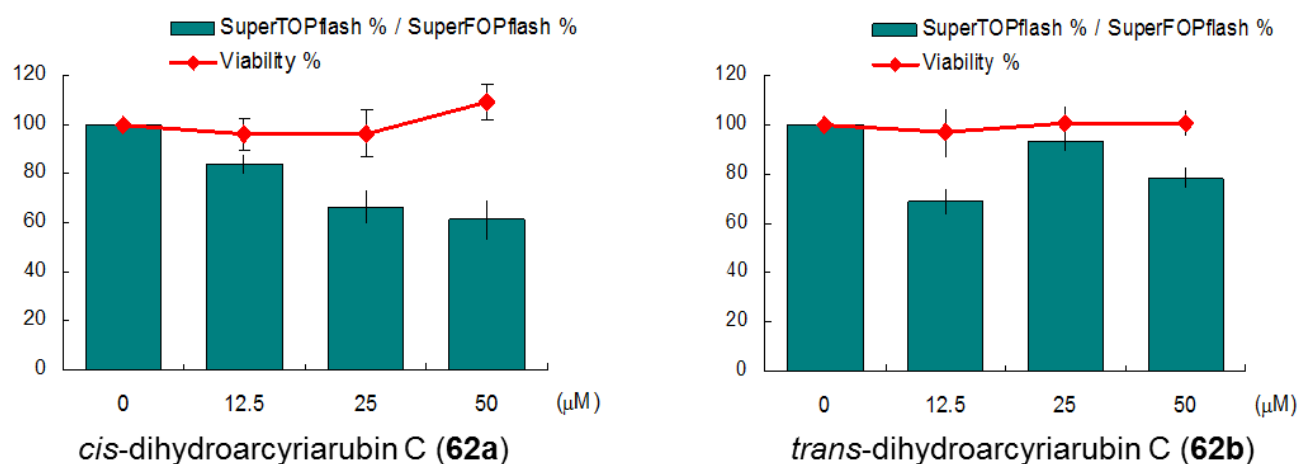


**Figure 18.** Wnt signal inhibitory activity of *cis*- and *trans*-dihydroarcyriarubin C (**62a** and **62b**)

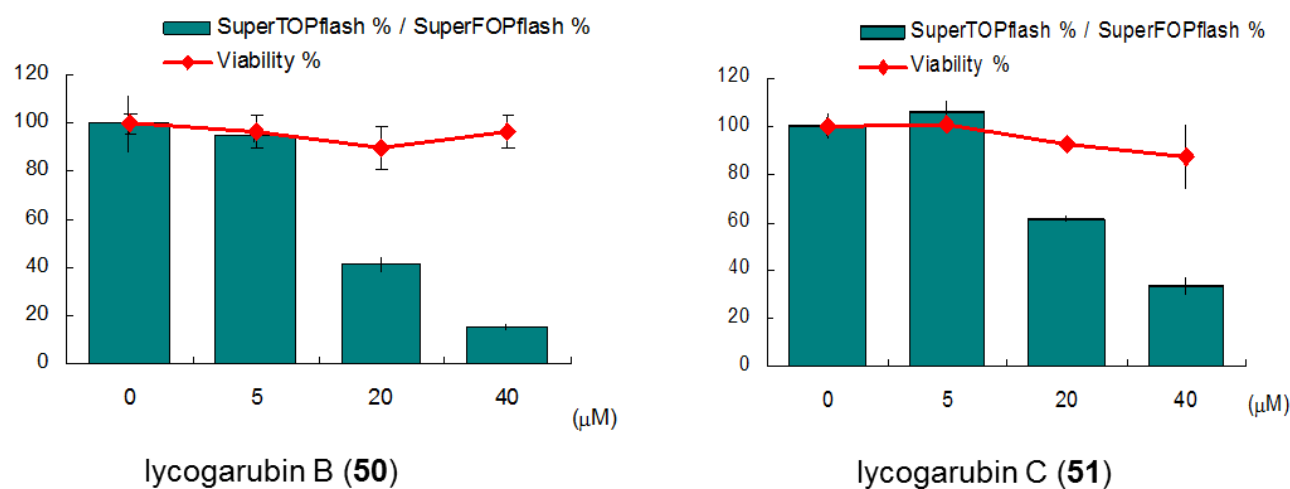


**Figure 19.** Wnt signal inhibitory activity of lycogarubins B (**50**) and C (**51**)

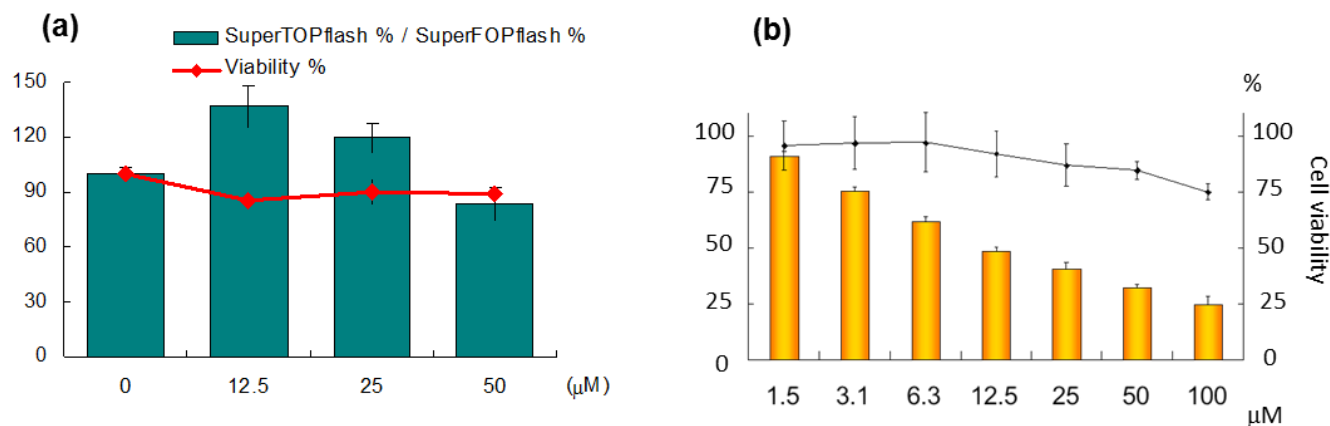
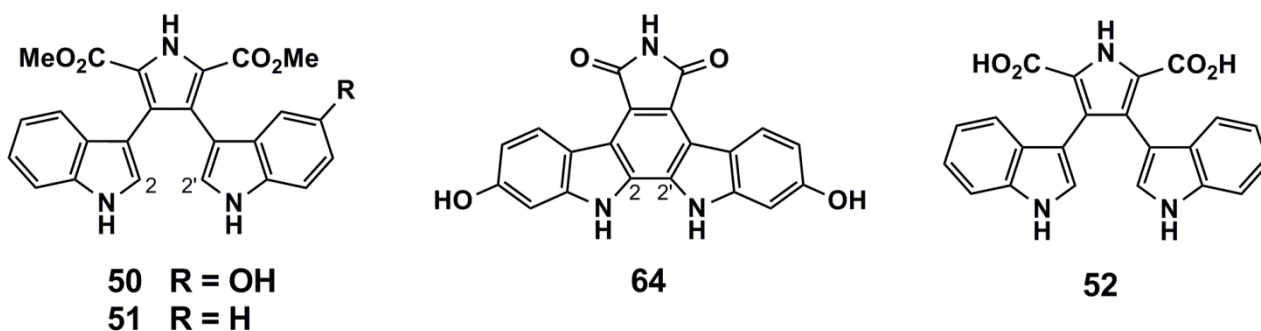


**Figure 20.** Wnt (a) and hedgehog (b) signal inhibitory activity of arcyriaflavin C (**64**)

exhibited dose-dependent hedgehog signal inhibition activity (Figure 20b).<sup>47</sup> Interestingly, lycogarubins B (**50**) and C (**51**) without a carbon-carbon bond between C-2 and C-2' positions did not show hedgehog signal inhibition activity. The presence or absence of the C-2/C-2' bond appears to be important for Wnt or hedgehog signal inhibition activity of bisindole alkaloids.



Lycogarinic acid (**52**) having a pyrrole dicarboxylic acid moiety, which we also isolated from *Lycogala epidendrum*,<sup>40</sup> was identified as an inhibitor of Hes1 dimer formation by our assay system using fluorophore-labeled Hes1 and Hes1 immobilized on microplates with an IC<sub>50</sub> value of 6.0 μM (Figure 21a).<sup>39</sup> We subsequently examined the intracellular inhibition activity of **52** by a cell-based reporter assay for measuring the effect on Hes1-induced repression in C3H10T1/2 cells. Decrease of luciferase activity to 35% in the reporter assay was observed in the presence of Hes1, since Hes1 suppresses the transcription of bHLH activators through homodimerization. Compound **52**, having an inhibition effect on Hes1 dimerization, showed dose-dependent inhibition of the Hes1-mediated suppression of gene expression; transcriptional activity assessed by reporter luciferase activity was recovered by compound **52** to around 60% at 50 μM (Figure 21b).

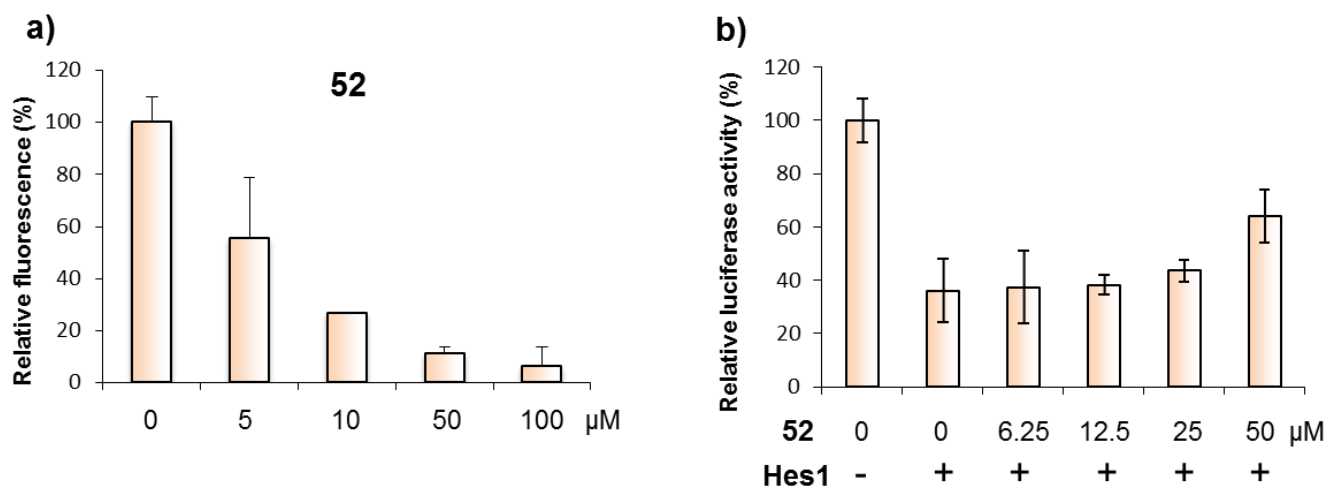


**Figure 21.** Hes1 inhibition activity of lycogaric acid (**52**). (a) Evaluation of the inhibitory activity of **52** on Hes1 dimer formation in a microplate. (b) Inhibitory effect of **52** on Hes1-dependent gene repression in C3H10T1/2 cells.

## 7. OTHER MYXOMYCETE CONSTITUENTS

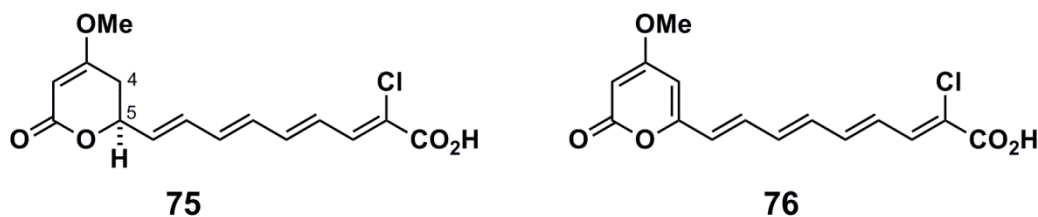
### (I) $\alpha$ -Pyrone with a chlorinated polyene acid

The fruit bodies of the myxomycete *Fuligo septica* f. *flava* (Figure 22), collected in Konan-shi, Kochi Prefecture, Japan, in 2008, were extracted with MeOH and acetone, and the combined extracts were subjected to repeated ODS and Sephadex LH-20 column chromatography to give two pigments, which were identified as new compounds, named fuligoic acid (**75**)<sup>52</sup> and dehydrofuligoic acid (**76**).<sup>53</sup> These new compounds were revealed to have an  $\alpha$ -pyrone structure with a chlorinated



**Figure 22.** Fruit bodies of *Fuligo septica* f. *flava*

tetraene carboxylic acid side chain by spectral data, including the CD data of **75**, suggesting its absolute configuration. Dehydrofuligoic acid (**76**) with one more unsaturation at the C-4/C-5 position had a longer conjugation than **75**, showing a yellow spot without spray reagent on TLC with longer UV absorption maxima [**75**:  $\lambda_{\max}$  340, 325, and 233 nm; **76**:  $\lambda_{\max}$  406, 386, and 303 nm]. Fuligoic acid (**75**) was inactive in our assay systems of Wnt, hedgehog, and TRAIL signaling pathways.



## (II) Naphthoquinone pigment

The fruit bodies of the myxomycete *Cribraria meylanii* (Figure 23), collected in Kami-shi, Kochi Prefecture, Japan, in 2007, were extracted with 90% MeOH and 90% acetone, and the combined extracts were subjected to chromatography on silica gel and ODS, followed by further purification with a Sephadex LH-20 column to give a dark red pigment compound, named cribrarione C (**77**).<sup>54</sup>

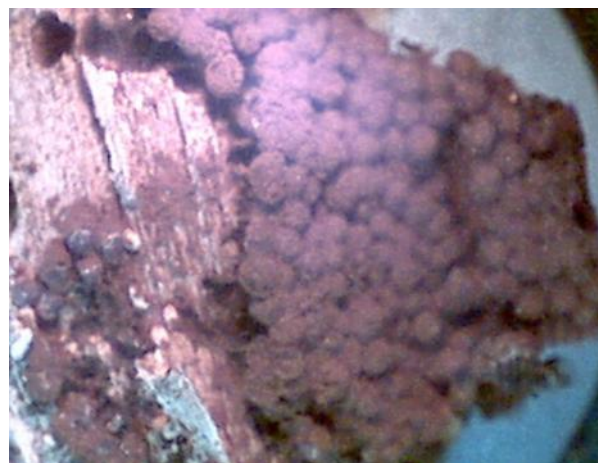
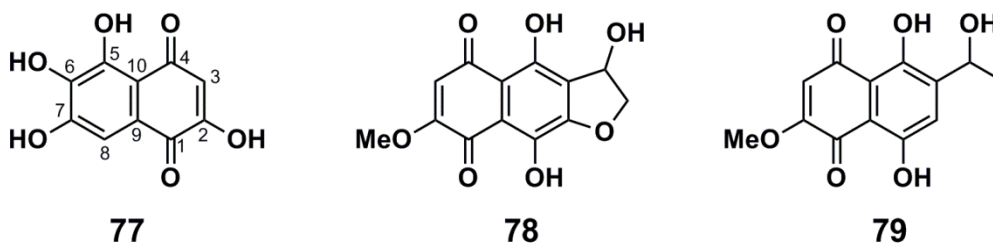


**Figure 23.** Fruit bodies of *Cribraria meylanii*

Its structure was elucidated by spectral data as 2,5,6,7-tetrahydroxy-1,4-naphthoquinone, which had been previously synthesized<sup>55</sup> and was first isolated as a natural product. We previously studied the pigment constituents of myxomycetes of the genus *Cribraria*, and isolated two naphthoquinone pigments; cribrarione A (**78**) from *Cribraria purpurea*<sup>56</sup> and cribrarione B (**79**) from *Cribraria cancellata*.<sup>57</sup> These naphthoquinones, as well as lindbladione (**41**) and its derivatives (**42-46**) isolated from *Lindbladia tubulina* (vide supra), are fine pigments, which may be one reason for the natural occurrence of these molecules.



The cytotoxicity of cribrarione C (**77**) was examined against HeLa cells, but it proved to be inactive ( $IC_{50}$  value,  $>100 \mu M$ ), while it showed mild TRAIL resistance-overcoming activity against TRAIL-resistant human gastric adenocarcinoma (AGS) cells. Treatment of the cells with TRAIL (100 ng/mL) alone or compound **77** (75  $\mu M$ ) alone resulted in only a slight decrease in cell viability (87% and 96%,

respectively), whereas treatment of the cells with compound **77** at 75  $\mu\text{M}$  in the presence of TRAIL (100 ng/mL) reduced cell viability to 71%, which was 16% and 25% more than TRAIL only or **77** only, respectively, suggesting possible synergism between the two agents.

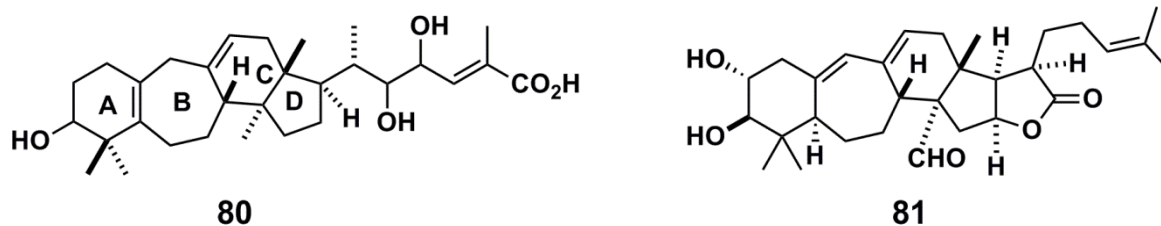
### (III) 9,10-Secocycloartane triterpenoid acid

The fruit bodies of the myxomycete *Tubulifera arachnoidea* (= *Tubifera ferruginosa*) (Figure 24), collected in Konan-shi, Kochi Prefecture, Japan, in 2008, were extracted with MeOH, and the EtOAc-soluble fraction of the MeOH extract was subjected to ODS column chromatography to give a new compound, tubiferic acid (**80**).<sup>58</sup> The structure of **80** was elucidated by spectral data as a triterpenoid having a consecutive 6-7-6-5 ring system with a 2,6-dimethyl-4,5-dihydroxy-2-hexenoic acid moiety as a side chain.



Figure 24. Fruit bodies of *Tubulifera arachnoidea*

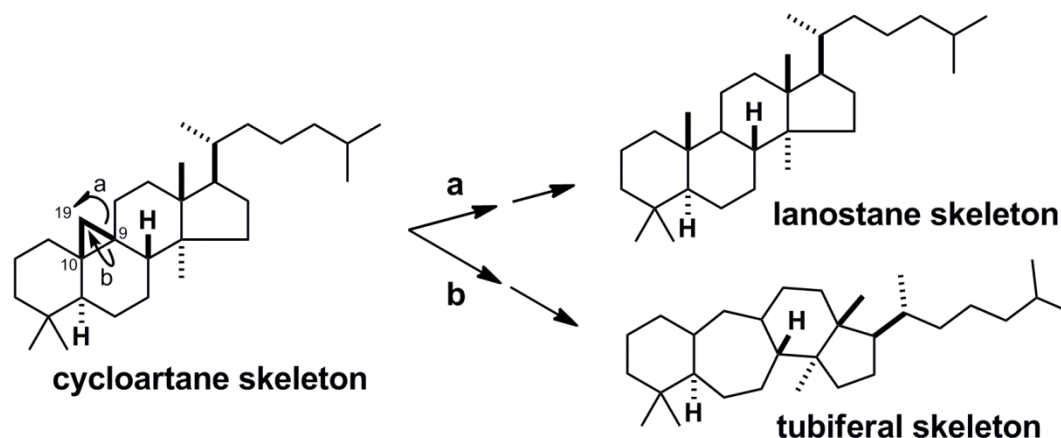
We previously studied the constituents of myxomycetes of the genus *Tubifera*, and isolated a triterpenoid aldehyde lactone, named tubiferal A (**81**), from *Tubifera dimorphotheca*.<sup>59</sup>



Tubiferic acid (**80**) had the same unique triterpenoid carbon skeleton as tubiferal A (**81**), and a potential biogenetic relationship with cycloartane and lanostane triterpene skeletons is shown in Scheme 9. We proposed that the stereochemistry of C/D rings of tubiferic acid (**80**) was parallel to that of tubiferal A (**81**) on the basis of NOE results, although the stereochemistry of a diol moiety in the side chain of **80** remained undefined. Since we could not obtain NOE correlations between A/B and C/D rings, their stereochemical relationship is arbitrary.

Tubiferal A (**81**) exhibited cytotoxicity against vincristine (VCR)-resistant human epidermoid carcinoma KB cells in the presence of VCR (100 ng/mL) with an  $\text{IC}_{50}$  value of 2.7  $\mu\text{g/mL}$ , while **81** was inactive in the absence of VCR, thus implying that tubiferal A (**81**) had a reversal effect on VCR resistance (more

than 4-fold) against VCR-resistant KB cell lines. Bioactivity of tubiferic acid (**80**) presently remains unexamined.



**Scheme 9.** Potential biogenetic relationship of tubiferal skeleton with cycloartane and lanostane skeletons.

## 8. CONCLUSION

Here we have described our recent studies on the isolation of bioactive natural products from myxomycetes, most of which have effects on the biological signaling pathways in our assay system including TRAIL, Wnt, Hes, and hedgehog signals. We have also described the synthesis of natural products and their related compounds with new structures. We are currently performing further comprehensive studies of natural product-based science,<sup>60</sup> called ‘chemical biology’, including i) signaling molecule-targeted screening of compounds from natural resources, such as plant materials collected from Thailand<sup>61</sup> and Bangladesh,<sup>62</sup> and actinomycetes<sup>63</sup> isolated from soil and sea water samples, ii) construction of a natural product-based synthetic compound library,<sup>64</sup> and iii) elucidation of the mechanism or target identification of selected bioactive compounds by analysis of mRNA and protein expression, and observation of the phenotypic changes in the cells, to discover and improve compounds applicable to drug development in the future.

## 9. ACKNOWLEDGEMENTS

We are grateful to Yukinori Yamamoto (Ohtsu-ko, Kochi) for collection of field specimens of myxomycetes. The research was supported by Grants in-Aid (22310133 and 23404007) for Scientific Research from the Japan Society for the Promotion of Science (JSPS), a Grant-in-Aid (23102008) for Scientific Research on Innovative Areas “Chemical Biology of Natural Products” from The Ministry of Education, Culture, Sports, Science and Technology, Japan (MEXT), Special Funds for Education and

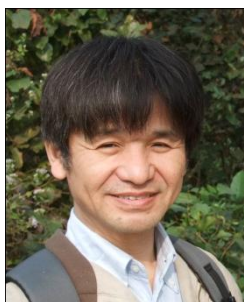
Research (Development of SPECT Probes for Pharmaceutical Innovation) from MEXT, the Iodine Research Project in Chiba University, Asian Core Program (JSPS), the Collaborative Research Program of the Institute for Chemical Research, Kyoto University (grant # 2011-45), and the Naito Foundation.

## 10. REFERENCES

1. D. J. Newman and G. M. Cragg, 'Natural Product Chemistry for Drug Discovery,' ed. by A. D. Buss and M. S. Butler, Royal Society of Chemistry, Cambridge, UK, 2010, pp. 3-27.
2. C. Gourmelon, J. S. Frenel, and M. Campone, *Expert Opin. Pharmacother.*, 2011, **12**, 2883.
3. J. Chun and V. Brinkmann, *Discov. Med.*, 2011, **12**, 213.
4. C. Pearce, P. Eckard, I. Gruen-Wollny, and F. G. Hansske, 'Natural Product Chemistry for Drug Discovery,' ed. by A. D. Buss and M. S. Butler, Royal Society of Chemistry, Cambridge, UK, 2010, pp. 215-241.
5. W. Steglich, *Pure Appl. Chem.*, 1989, **61**, 281.
6. T. Hashimoto, A. Yasuda, K. Akazawa, S. Takaoka, M. Tori, and Y. Asakawa, *Tetrahedron Lett.*, 1994, **35**, 2559.
7. M. Ishibashi, *Yakugaku Zasshi*, 2007, **127**, 1369.
8. M. Ishibashi, *Med. Chem.*, 2005, **1**, 575.
9. M. Ishibashi, 'Studies in Natural Products Chemistry,' Vol. 29, ed. by Atta-ur-Rahman, Elsevier Science, Amsterdam, 2003, pp. 223-262.
10. V. M. Dembitsky, T. Rezanka, J. Spizek, and L. O. Hanus, *Phytochemistry*, 2005, **66**, 747.
11. M. Ishibashi and M. A. Arai, *J. Synth. Org. Chem. Jpn.*, 2009, **67**, 1094.
12. M. Ishibashi and T. Ohtsuki, *Med. Res. Rev.*, 2008, **28**, 688.
13. S. Nakatani, Y. Yamamoto, M. Hayashi, K. Komiyama, and M. Ishibashi, *Chem. Pharm. Bull.*, 2004, **52**, 368.
14. X. Wu, Y. Liu, W. Sheng, J. Sun, and G. Qin, *Planta Medica*, 1997, **63**, 55.
15. H. Hasegawa, Y. Yamada, K. Komiyama, M. Hayashi, M. Ishibashi, T. Yoshida, T. Sakai, T. Koyano, T.-S. Kam, K. Murata, K. Sugahara, K. Tsuruda, N. Akamatsu, K. Tsukasaki, M. Masuda, N. Takasu, and S. Kamihira, *Blood*, 2006, **107**, 679.
16. H. Hasegawa, Y. Yamada, K. Komiyama, M. Hayashi, M. Ishibashi, T. Sunazuka, T. Izuhara, K. Sugahara, K. Tsuruda, M. Masuda, N. Takasu, K. Tsukasaki, M. Tomonaga, and S. Kamihira, *Blood*, 2007, **110**, 1664.
17. S. S. More, D. Shanmughapriya, Y. Lingam, and N. B. Patel, *Synth. Commun.*, 2009, **39**, 2058.
18. B. Pettersson, V. Hasimbegovic, and J. Bergman, *Tetrahedron Lett.*, 2010, **51**, 238.
19. M. A. Arai, J. Seto, F. Ahmed, K. Uchiyama, and M. Ishibashi, *Synlett*, 2010, 2498.

20. After our synthesis, Bergman *et al.* also obtained fuligocanding B in optically active form: B. Pettersson, V. Hasimbegovic, and J. Bergman, [\*J. Org. Chem.\*, 2011, \*\*76\*\*, 1554.](#)
21. R. K. Srivastava, [\*Neoplasia\*, 2001, \*\*3\*\*, 535.](#)
22. F. Ahmed, K. Toume, S. K. Sadhu, T. Ohtsuki, M. A. Arai, and M. Ishibashi, [\*Org. Biomol. Chem.\*, 2010, \*\*8\*\*, 3696.](#)
23. E. Lindhagen, P. Mygren, and R. Larsson, [\*Nature Protocols\*, 2008, \*\*3\*\*, 1364.](#)
24. M. Ishibashi, T. Iwasaki, S. Imai, S. Sakamoto, K. Yamaguchi, and A. Ito, [\*J. Nat. Prod.\*, 2001, \*\*64\*\*, 108.](#)
25. S. Nakatani, K. Kamata, M. Sato, H. Onuki, H. Hirota, J. Matsumoto, and M. Ishibashi, [\*Tetrahedron Lett.\*, 2005, \*\*46\*\*, 267.](#)
26. S. Hanazawa, M. A. Arai, X. Li, and M. Ishibashi, [\*Bioorg. Med. Chem. Lett.\*, 2008, \*\*18\*\*, 95.](#)
27. M. A. Arai, Y. Uchino, S. Hanazawa, X. Li, N. Kimura, and M. Ishibashi, [\*Heterocycles\*, 2008, \*\*76\*\*, 1425.](#)
28. J.-M. Luo, C.-F. Dai, S.-Y. Lin, and P.-Q. Huang, [\*Chem. Asian J.\*, 2009, \*\*4\*\*, 328.](#)
29. M. A. Arai, S. Hanazawa, Y. Uchino, X. Li, N. Kimura, and M. Ishibashi, *Org. Biomol. Chem.*, 2010, **8**, 5285.
30. X. Li, T. Ohtsuki, T. Koyano, T. Kowithayakorn, and M. Ishibashi, [\*Chem. Asian J.\*, 2009, \*\*4\*\*, 540.](#)
31. N. Mori, K. Toume, M. A. Arai, T. Koyano, T. Kowithayakorn, and M. Ishibashi, [\*J. Nat. Med.\*, 2011, \*\*65\*\*, 234.](#)
32. S. Angers and R. T. Moon, *Nat. Rev. Mol. Cell Biol.*, 2009, **10**, 468.
33. J. C. Curtin and M. V. Lorenzi, *Oncotarget*, 2010, **1**, 552.
34. H. Yao, E. Ashihara, and T. Maekawa, [\*Expert Opin. Ther. Targets\*, 2011, \*\*15\*\*, 873.](#)
35. F. Verkaar and G. J. R. Zaman, [\*Drug Discov. Today\*, 2011, \*\*16\*\*, 35.](#)
36. W. Steglich, [\*Pure Appl. Chem.\*, 1989, \*\*61\*\*, 281.](#)
37. Y. Ishikawa, M. Ishibashi, Y. Yamamoto, M. Hayashi, and K. Komiyama, [\*Chem. Pharm. Bull.\*, 2002, \*\*50\*\*, 1126.](#)
38. Y. Misono, Y. Ishikawa, Y. Yamamoto, M. Hayashi, K. Komiyama, and M. Ishibashi, [\*J. Nat. Prod.\*, 2003, \*\*66\*\*, 999.](#)
39. M. A. Arai, A. Masada, T. Ohtsuka, R. Kageyama, and M. Ishibashi, [\*Bioorg. Med. Chem. Lett.\*, 2009, \*\*19\*\*, 5778.](#)
40. R. Kageyama, T. Ohtsuka, and T. Kobayashi, [\*Development\*, 2007, \*\*134\*\*, 1243.](#)
41. T. Hosoya, Y. Yamamoto, Y. Uehara, M. Hayashi, K. Komiyama, and M. Ishibashi, [\*Bioorg. Med. Chem. Lett.\*, 2005, \*\*15\*\*, 2776.](#)
42. T. Hashimoto, A. Yasuda, K. Akazawa, S. Takaoka, M. Tori, and Y. Asakawa, [\*Tetrahedron Lett.\*](#)

- [1994, 35, 2559](#).
43. R. Fröde, C. Hinze, I. Josten, B. Schmidt, B. Steffan, and W. Steglich, [Tetrahedron Lett., 1994, 35, 1689](#).
  44. T. Yasuzawa, T. Iida, M. Yoshida, N. Hirayama, M. Takahashi, K. Shirahata, and H. Sano, [J. Antibiot., 1986, 39, 1072](#).
  45. K. Kamata, M. Kiyota, A. Naoe, S. Nakatani, Y. Yamamoto, M. Hayashi, K. Komiyama, T. Yamori, and M. Ishibashi, [Chem. Pharm. Bull., 2005, 53, 594](#).
  46. A. Shintani, K. Toume, Y. Rifai, M. A. Arai, and M. Ishibashi, [J. Nat. Prod., 2010, 73, 1711](#).
  47. T. Hosoya, M. A. Arai, T. Koyano, T. Kowithayakorn, and M. Ishibashi, [ChemBioChem, 2008, 9, 1082](#).
  48. N. Takebe, P. J. Harris, R. Q. Warren, and S. P. Ivy, [Nat. Rev. Clin. Oncol., 2011, 8, 97](#).
  49. S. Nakatani, A. Naoe, Y. Yamamoto, T. Yamauchi, N. Yamaguchi, and M. Ishibashi, [Bioorg. Med. Chem. Lett., 2003, 13, 2879](#).
  50. K. Kaniwa, M. A. Arai, X. Li, and M. Ishibashi, [Bioorg. Med. Chem. Lett., 2007, 17, 4254](#).
  51. M. Ohkubo, T. Nishimura, H. Jona, T. Honma, and H. Morishima, [Tetrahedron, 1996, 52, 8099](#).
  52. A. Shintani, T. Ohtsuki, Y. Yamamoto, T. Hakamatsuka, N. Kawahara, Y. Goda, and M. Ishibashi, [Tetrahedron Lett., 2009, 50, 3189](#).
  53. A. Shintani, K. Toume, Y. Yamamoto, and M. Ishibashi, [Heterocycles, 2010, 82, 839](#).
  54. A. Shintani, H. Yamazaki, Y. Yamamoto, F. Ahmed, and M. Ishibashi, [Chem. Pharm. Bull., 2009, 57, 894](#).
  55. S. Natori and Y. Kumada, [Chem. Pharm. Bull., 1965, 13, 1472](#).
  56. A. Naoe, M. Ishibashi, and Y. Yamamoto, [Tetrahedron, 2003, 59, 3433](#).
  57. D. Iwata, M. Ishibashi, and Y. Yamamoto, [J. Nat. Prod., 2003, 66, 1611](#).
  58. Y. Ippongi, T. Ohtsuki, K. Toume, M. A. Arai, Y. Yamamoto, and M. Ishibashi, [Chem. Pharm. Bull., 2011, 59, 279](#).
  59. K. Kamata, H. Onuki, H. Hirota, Y. Yamamoto, M. Hayashi, K. Komiyama, M. Sato, and M. Ishibashi, [Tetrahedron, 2004, 60, 9835](#).
  60. M. A. Arai, [Chem. Pharm. Bull., 2011, 59, 417](#).
  61. M. A. Arai, C. Tateno, T. Koyano, T. Kowithayakorn, S. Kawabe, and M. Ishibashi, [Org. Biomol. Chem., 2011, 9, 1133](#).
  62. F. Ahmed, S. K. Sadhu, and M. Ishibashi, [J. Nat. Med., 2010, 64, 393](#).
  63. M. S. Abdelfattah, K. Toume, and M. Ishibashi, [J. Antibiot., 2011, 64, 729](#).
  64. M. A. Arai, M. Sato, K. Sawada, T. Hosoya, and M. Ishibashi, [Chem. Asian J., 2008, 3, 2056](#).



**Masami Ishibashi** received his Ph.D. in chemistry at University of Tokyo in 1985 (under Prof. Takeyoshi Takahashi), and he worked as a postdoctoral fellow at University of Hawaii (with Prof. Richard E. Moore), Mitsubishi-Kasei Institute of Life Sciences (with Prof. Jun'ichi Kobayashi and Yasushi Ohizumi), and Kitasato Institute (with Prof. Satoshi Ōmura and Kanki Komiyama). He joined the faculty of Toho University in 1989 (with Prof. Michiko Iwamura), and moved to Hokkaido University as an associate professor in 1990 (with Prof. Jun'ichi Kobayashi). He has been a full professor of natural products chemistry at Graduate School of Pharmaceutical Sciences, Chiba University since 1997, where he still continues his research career in the field of natural products chemistry. In 2007, he received the Pharmaceutical Society of Japan Award for Divisional Scientific Promotions.



**Midori A. Arai** received his Ph.D. at University of Tokyo in 2000 (under Prof. Masakatsu Shibasaki), and she worked as a postdoctoral fellow at Osaka University (with Prof. Hiroaki Sasai), Harvard University (with Prof. Stuart L. Schreiber), and RIKEN (with Prof. Yukishige Ito). She joined the faculty of Teikyo University as an assistant professor in 2004 (with Prof. Atsushi Kittaka), and moved to Chiba University as an associate professor in 2007 (-present). She was a visiting associate professor at Institute for Chemical Research, Kyoto University (2010-2011). She received the Sankyo Award in Synthetic Organic Chemistry, Japan in 2001, the Pharmaceutical Society of Japan Award for Young Scientists in 2010, and the Association of University Women Morita Award for Scientific Research in 2011.